Deep-sea response to interglacial-glacial variability on the South Australian margin over the last 94 ka

Robin Fentimen, P de Deckker, Pauline Depuydt, Meryem Mojtahid

Quaternary Science Reviews 320 (2023) 108328

Contents lists available at ScienceDirect

Quaternary Science Reviews

journal homepage: www.elsevier.com/locate/quascirev

Deep-sea response to interglacial-glacial variability on the South Australian margin over the last 94 ka

R. Fentimen [a,*], P. De Deckker [b], P. Depuydt [a,c], M. Mojtahid [a]

[a] Université D'Angers, Nantes Université, Le Mans Université, CNRS, Laboratoire de Planétologie et Géosciences, LPG UMR 6112, 49000, Angers, France
[b] Research School of Earth Sciences, The Australian National University, Canberra ACT, 2601, Australia
[c] GEOPS, Universities of Paris Sud and Paris-Saclay, CNRS, 91405, Orsay, France

ARTICLE INFO

Handling Editor: A. Voelker

Keywords:
Benthic foraminifera
Palaeoceanography
Marine isotope stages
Bottom currents
Deep boundary current
Continental slope
Canyons
Antarctic bottom water

ABSTRACT

The continuous record offered by deep-sea sediments has been extensively used to constrain shifting continental and oceanographic conditions. Yet, past fluctuations in deep-sea benthic conditions and bottom-currents are in numerous parts of the globe scarcely documented, one such example being the South Australian margin. Indeed, though variations in surface water masses and continental aeolian dust and river outflow are well documented in the area, little is known about benthic environments and their dynamics during the last interglacial-glacial cycle. We focus here on benthic foraminiferal assemblages sampled from a sediment core recovered at 2420 m depth from a small plateau south of Kangaroo Island within the underwater Murray Canyons Group (South Australian margin). Benthic foraminiferal assemblages show a distinct separation between interglacial and glacial periods over the last 94 ka, and indicate that the benthic environment was well-ventilated and oligotrophic during glacial periods, whilst being rather marked by reduced oxygenation associated to higher food input during the Holocene and Marine Isotope Stage 5a-c. We demonstrate that autochtonous deep-sea benthic foraminiferal communities neither respond to changes in the Murray River's discharges, nor do they follow variations in aeolian dust input from South Australia. Instead, the deep-sea and the terrestrial realm appear decoupled. Moreover, our observations suggest that bottom-water slope currents were stronger during the Holocene and Marine Isotope Stage 5a-c. We propose that this strengthening was triggered by an intensification of the poleward-circulating deep eastern boundary current transporting carbon-rich Indian Deep Water. In contrast, glacial seafloor conditions, especially during the Last Glacial Maximum, may reflect a greater influence and a shoaling of oxygen-rich Antarctic Bottom Water of South Australia. This bottom-water shift would follow the northward displacement of the Subtropical and Subantarctic Fronts and coincide with a withering influence of the Leeuwin Current within surface waters.

1. Introduction

The Quaternary is marked by a rapid succession of cold glacial and warm interglacial periods. Temperature changes reached an amplitude of over 15 °C in some parts of the world (e.g., Antarctica and the Arctic; Jouzel et al., 2007; Miller et al., 2010) with a regular waxing and waning of ice sheets and continental glaciers (Lowe and Walker, 2014). Hence, continental conditions rapidly shifted from arid to damp/wet conditions (Pye, 1995; Cohen et al., 2022), whilst oceanic circulation also underwent profound changes (Bassinot et al., 1994; Seidov and Haupt, 1997; Kuijpers et al., 2003; Singh et al., 2023). The Quaternary long-term climate variability is governed by variations in the earth's orbit and axis (Hays et al., 1976; Imbrie et al., 1993; Bassinot et al., 1994), which control the amount of radiation and the heat distribution received by the earth's surface (Lowe and Walker, 2014). However, orbital forcing cannot solely explain global climatic changes during the Quaternary, as evidenced by shifts in the periodicity of orbital cycles, the most emblematic being the Mid-Pleistocene Revolution (Berends et al., 2021). Other drivers such as tectonic activity and feedback mechanisms induced by ocean, atmosphere and cryosphere interactions also play a key role (Denton, 2000; Stott et al., 2007; Skinner et al., 2010). Noticeable large amplitude rapid climatic fluctuations superimposed to these long-term climatic variations, such as Heinrich and Dansgaard-Oeschger events, are well preserved in ice, marine and

* Corresponding author.
E-mail address: robin.fentimen@univ-angers.fr (R. Fentimen).

https://doi.org/10.1016/j.quascirev.2023.108328
Received 23 June 2023; Received in revised form 21 September 2023; Accepted 21 September 2023
Available online 27 October 2023

terrestrial archives (e.g., Blunier and Brook, 2001; Magee et al., 2004; Moine et al., 2008; Barker et al., 2009).

Deep-sea sediments have been widely used to unravel these varying oceanic and continental environmental conditions since they can offer continuous long-lasting time windows, and record the coupling between terrestrial, surface, and deep ocean environments (Corliss et al., 1986; Lisiecki and Raymo, 2005). Off the South Australian margin, this approach has noticeably been used on two marine sediment cores (MD03-2607, MD03-2611; Fig. 1), recovered south of Kangaroo Island from the slope of the Murray Canyons Group (AUSCAN cruise; https://doi.org/10.17600/3200090), to quantify and identify the fluctuating provenance of fluvial material and aeolian dust as well as vegetation on land since the last interglacial period (Hill and De Deckker, 2004; Gingele et al., 2004, 2007; Gingele and De Deckker, 2005; De Deckker et al., 2020). The same two cores also allowed for a detailed reconstruction of surface-water mass dynamics and continental changes since the last interglacial period (De Deckker et al., 2012, 2019, 2020, 2021; Moros et al., 2009, 2021). However, most of these studies along the South Australian margin investigated sedimentary and surface water characteristics, whilst little is yet known about the response of deep-sea ecosystems to the documented changes happening within surface waters and inland since the last interglacial period. To fill this knowledge gap, we have investigated benthic foraminiferal assemblages from core MD03-2611 (Fig. 1) recovered at a depth of 2420 m and presenting a continuous sedimentary record for the last 94 ka. This core has previously been studied using several proxies, including planktic foraminiferal assemblages, to constrain the variability of shallow ocean currents and the migration of oceanic fronts, such as the Leeuwin Current (LC) and the Subtropical and Subantarctic Fronts (Fig. 1) (De Deckker et al., 2012, 2019, 2020; Moros et al., 2009, 2021; Perner et al., 2018).

Benthic foraminifera are widely used to reconstruct past marine environments, from coastal waters to the deep-sea realm (e.g., ; Alve, 1991; Cann et al., 1993; Schönfeld and Zahn, 2000; Schmiedl et al., 2003; Durand et al., 2016), since they are ubiquitous in the marine domain, in addition to being highly diversified and densely distributed (Murray, 2006). Moreover, they generally fossilize remarkably well due to their robust tests consisting of calcium carbonate or agglutinated material. Foraminifera make up 25% of the ocean's present-day carbonate production (Langer, 2008), whilst foraminiferal (planktic and benthic) ooze composes a considerable amount of the ocean's seafloor sediments (Dutkiewicz et al., 2015) and is hence an ideal archive of past ocean dynamics. The usefulness of fossil benthic foraminifera as indicators of past seafloor conditions depends on our understanding of living communities. In the deep-sea, the composition and distribution of living benthic foraminiferal faunas are essentially governed by the quantity and quality of food reaching the seafloor (e.g., Gooday, 1993; Jorissen et al., 2007; Fontanier et al., 2008) and by oxygen concentrations, noticeably in the sediment pore-water (e.g., Jorissen et al., 1995;

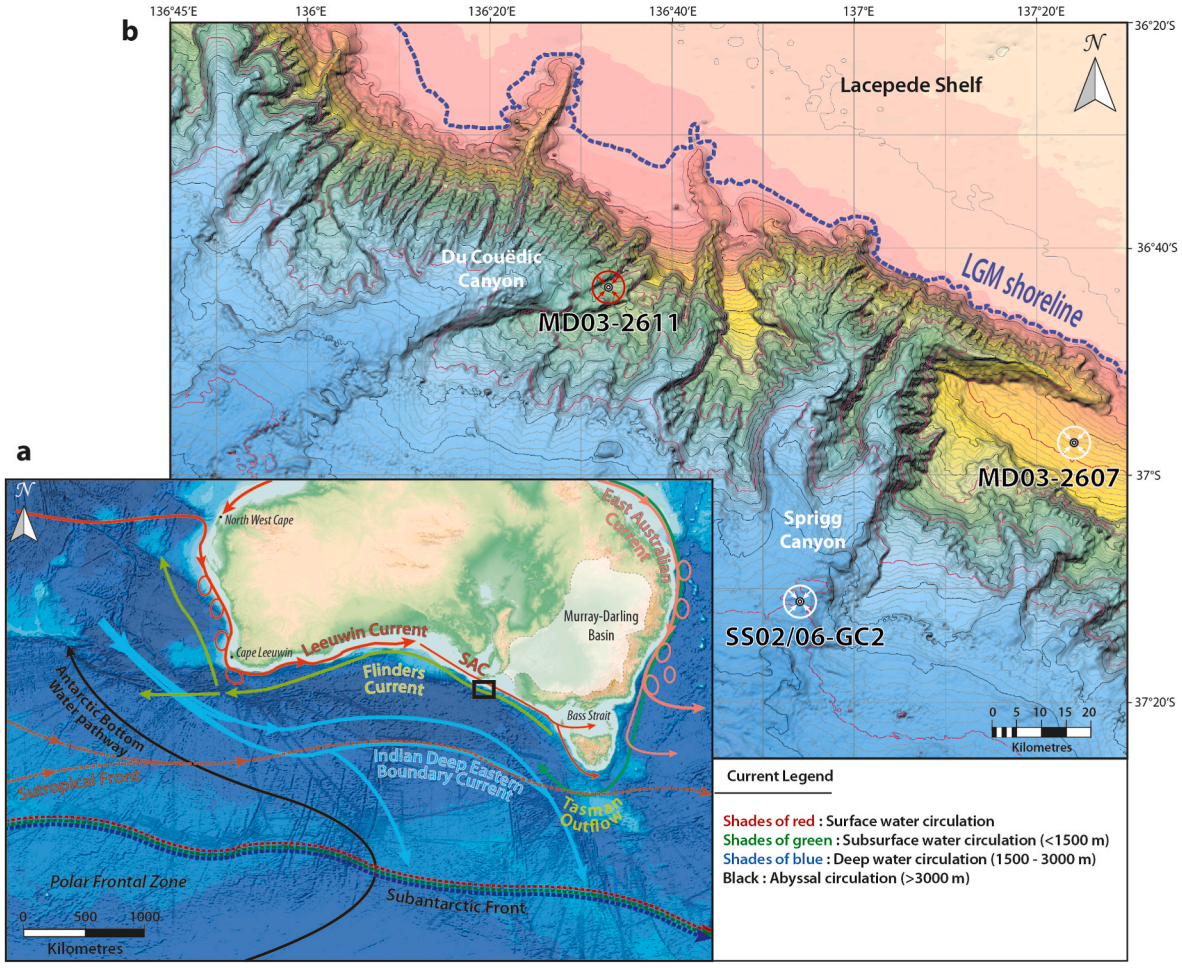

Fig. 1. a) Map of oceanic circulation offshore southern Australia (based on GEBCO data) showing the main surface, intermediate, and deep-water masses. The circulation of water currents follows the descriptions given by Middleton and Bye (2007), Tamsitt et al. (2019), and Duran et al. (2020). SAC: South Australian Current. The geographical extent of the Murray–Darling Basin is shown after Hill et al. (2009). b) Bathymetric map of the study area (close-up of the black rectangle in (a)): approximate Last Glacial Maximum (LGM) palaeoshoreline, and location of core MD03-2611 (red circle), occurring on a promontory, and of cores MD03-2607 and SS02/06-GC2 (white circles). Courtesy of Peter Hill and using multibeam data acquired during the AUSCAN survey in 2003 (Hill and De Deckker, 2004). The Lacepede Shelf (shades of pink) extends down to 200 m. 1000 m contour lines are in red.

Gooday, 2019), which are in turn influenced by oceanographic regimes. Temperature, in contrast with coastal environments, is relatively uniform at greater depths and has hence only a minor impact on foraminiferal distribution (Gooday and Jorissen, 2012). Though commonly associated with intertidal environments, tides and currents, such as internal waves propagating at the boundary between water masses and upwelling/downwelling currents, can also control benthic foraminiferal distribution at great depths (e.g, Sen Gupta et al., 1981; Schönfeld, 1997; Diz et al., 2006; Fentimen et al., 2021). Strong turbulence favours the development of epibenthic species, living at the sediment surface or attached to elevated substrates where food availability is enhanced (e.g., Schönfeld, 1997; 2011; Fentimen et al., 2021). Benthic foraminifera are not limited to the surface but also colonize microhabitats at depths down to approximately 10 cm within the sediment (e.g., Fontanier et al., 2008; Jorissen et al., 2007). The distribution of these infaunal species is controlled by food and oxygen availability at depth, with some deep-dwelling species able to sustain severe oxygen depletion (e.g., Jorissen et al., 1995; Fontanier et al., 2005; Murgese and De Deckker, 2005). Knowledge of modern deep-sea benthic foraminiferal assemblages along the South Australian continental slope is scarce. Studies have primarily concentrated on the continental shelf (Chapman, 1907; Parr, 1932; Cann et al., 1993; Li et al., 1996; Nash et al., 2010), with two exceptions being the study of living benthic foraminifera by Basak et al. (2009) at two sites collected offshore Southern Australia during the AUSCAN cruise in the vicinity of the core studied here, and the investigation of living and dead foraminifera by Smith and Gallagher (2003) from grab samples retrieved along a transect in the Bass Canyon (Southeast Australia) between approximately 80 and 3700 m depth. In addition, Willingham (2014) noted a predominance of living infaunal species in two surface samples situated at approximately 1100 m depth at 140°E. Modern deep-sea benthic foraminiferal assemblages have been better investigated in the eastern Indian Ocean off the eastern coast of Australia (Peterson, 1984; Rathburn and Corliss, 1994; Murgese and De Deckker, 2005) and within the shallow and deep waters around New Zealand (Hayward et al., 1997, 1999, 2010), with also some sparse studies conducted along the West Australian margin (Quilty and Hosie, 2006; Schröder-Adams et al., 2008). Similarly, there are few studies documenting downcore fossil benthic foraminiferal assemblages along the South Australian margin (Passlow et al., 1997; Nees et al., 1999; Nash et al., 2018; Mojtahid et al., 2020). For instance, the recent study of Mojtahid et al. (2020) on core SS0/06-GC2, retrieved from the abyssal part of the Murray Canyons Group (Fig. 1), used deep-sea benthic foraminiferal assemblages to determine the origin of turbidites within the sedimentary record. However, this turbiditic record, being discontinuous, did not allow for a reconstruction of the deep-sea ecosystem and how it responds to glacial-interglacial climate changes. As such, core MD03-2611 offers the opportunity to considerably broaden our knowledge of deep-sea fossil benthic foraminiferal assemblages off southern Australia and to answer the following scientific questions:

i) How do benthic foraminifera, as deep-sea biological indicators, integrate the cumulative impacts of changing physical habitats and surface water characteristics during glacial-interglacial climate conditions?
ii) How can the joint investigation of benthic and planktic communities help us disentangle oceanic and continental forcing on orbital and sub-orbital timescales?

2. Regional setting

2.1. Geographical setting

The Murray Canyons Group is a remarkable system of under-water canyons extending from the shelf break down to 5000 m depth (Fig. 1; Sprigg, 1948; Hill and De Deckker, 2004; Hill et al., 2005). The continental shelf in the vicinity of Kangaroo Island, namely the Lacepede Shelf (Fig. 1), is more than 150 km wide and lies on average at 30–80 m depth (Hill and De Deckker, 2004; James and Bone, 2011). It is a highly productive area driven by summer and autumn upwelling of cool nutrient-rich waters (Lewis, 1981; Ward et al., 2006; James and Bone, 2011; Richardson et al., 2020). On the Great Australian Bight, Van Ruth et al. (2018) reported peak NO_x concentrations between 3 and 10 μM. These values are higher than concentrations documented off south-west Western Australia (2–6 μM; Hanson et al., 2005), yet lower than those documented for the major eastern boundary current upwelling regions off Peru, north-west Africa, and California (15–19 μM; Messié et al., 2009). Thus, Van Ruth et al. (2018) conclude that, on a global scale, the eastern Great Australian Bight may be considered a region subject to moderate enrichment.

The slope, in contrast to the near to flat shelf, drops 3500 m over a horizontal distance of 25 km, with slopes as steep as 25°–30° (Fig. 1; Hill and De Deckker, 2004). The Murray Canyons are situated off the Murray River mouth, which is the termination of the Murray-Darling fluvial system that covers approximately 1/7th of the Australian continent, i.e. an area in excess of 1,000,000 km^2 (Fig. 1; Gingele and De Deckker, 2005). The Murray-Darling catchment is fuelled by monsoonal precipitation in the north during the austral summer and rainfall delivered by the westerlies in the south, mostly during the austral winter. Material transported by the Murray-Darling fluvial system together with aeolian dust originating from the Australian continent may be deposited at depth on the continental slope (Gingele et al., 2004, 2007; Gingele and De Deckker, 2005). The proximity of the Murray River mouth to the Murray Canyons is governed by glacial-interglacial sea-level fluctuations (Fig. 1b; Gingele et al., 2004). Today's high sea-level and modern human interferences result in a near-absence of river input on the continental slope (Gingele and De Deckker, 2005). Yet, during periods of low-sea levels, noticeably during the Last Glacial Maximum (LGM), river input increased due to the proximity of the Murray River mouth and deposited quartzose sands on the Lacepede Shelf (Fig. 1b; James et al., 1992; Gingele et al., 2004; Hill et al., 2009; James and Bone, 2011). At present, deep neritic (100–200 m depth) and slope environments nearly only consist of recent carbonate sediments (James and Bone, 2011). Sediments on the abyssal plain (ca. 5000 m depth) are made up of calcareous ooze (Dutkiewicz et al., 2015) but also red clay with a good preservation of foraminifera in turbiditic sequences that preserve carbonates (Mojtahid et al., 2020).

2.2. Modern oceanography

Surface waters flowing along the South Australian coastline originate in the Indian Ocean and flow east along Australia, reaching western Tasmania (Cresswell and Domingues, 2009; Wijffels et al., 2018). These high temperature (10–22 °C) and high salinity (35.1–35.9) waters, referred to as Subtropical Surface Water, circulate approximately between 0 and 250 m depth (James and Bone, 2011; Wijffels et al., 2018; Richardson et al., 2019). Subantarctic Mode Water, a water mass high in dissolved oxygen and formed from deep winter convection within the Subantarctic Zone, is found below surface waters between 350 and 750 m depth (McCartney, 1977, 1982; James and Bone, 2011). Intermediate depths between 750 and 1200 m are bathed by Antarctic Intermediate Water, a low salinity body extending just north of the Subantarctic Front (Piola and Georgi, 1982; James and Bone, 2011; Yao and Shi, 2017). Circumpolar Deep Water and underlying Antarctic Bottom Water (AABW) make up the deep water masses from approximately 1200 m depth down to the seafloor (Osborn et al., 1983; Passlow et al., 1997). Circumpolar Deep Water can be divided between an upper (1200–1600 m) and a lower (1600–4000 m) part, with the latter being colder and higher in salinity (Passlow et al., 1997). Antarctic Bottom Water is sourced essentially from the Weddell Sea (60%), and to a lesser extent from the Ross Sea and Mertz Polynya region (Rintoul, 1998; Orsi et al., 2002), and spreads into the Australian Antarctic Basin towards the west of southern Australia (Aoki et al., 2020 and references therein; Fig. 1).

Antarctic Bottom Water is found below 4000 m depth within south-eastern Australian waters (Passlow et al., 1997).

The ca. top 200 m of the water column is affected by the Leeuwin Current (LC), which circulates eastward along the shelf from North West Cape (Western Australia) to the Great Australian Bight (Ridgway and Condie, 2004) (Fig. 1). The LC is derived from Indonesian Throughflow, an outflow of western Pacific Ocean waters passing through the Indonesian archipelagos, and is noticeably warm, low salinity and oligotrophic (Cresswell and Domingues, 2009). Addition of subtropical waters east and southward lowers the LC's temperature and increases its salinity and density (Cresswell and Griffin, 2004). At present, the influence of LC is more prominent during la Niña events in the austral winter period from May to October when it reaches as far east as 124°E (Rochford, 1986; Ridgway and Condie, 2004; Wijffels et al., 2018) and where it is then substituted by the South Australian Current that reaches to the Bass Strait in the West (Ridgway and Condie, 2004; Richardson et al., 2019). The strength of the LC varies in time, a striking example being its weakness during the LGM (De Deckker et al., 2012). Situated below the LC and circulating in the opposite direction (westward) between 400 and 800 m, the Flinders Current (FC) reaches average flow velocities of ca. 8 cm s^{-1} and appears to be restricted to the slope (Middleton and Cirano, 2002; Middleton and Bye, 2007). Similar to the LC, the FC is the strongest and most continuous in spring and summer and is reinforced in the west (Middleton and Bye, 2007; Richardson et al., 2019). The FC transports Subantarctic Mode Water together with Tasman Outlow waters in the far southeast (Fig. 1; Cirano and Middleton, 2004; Richardson et al., 2019). In addition to these shallow currents, Tamsitt et al. (2019) found evidence of a deep boundary current (i.e., Indian Deep Eastern Boundary Current, Fig. 1a) flowing eastward to the south of Australia and at depths between 1500 and 3000 m. The water mass transported by this deep boundary current matches the low-oxygen, carbon rich signature of Indian Deep Water from the eastern Indian Ocean (McDonagh et al., 2008; Tamsitt et al., 2019).

3. Material and methods

3.1. Core material, age model and previous work

The 11.97 m long sediment core MD03-2611 was collected during the AUSCAN cruise in 2003 on-board the research vessel *Marion Dufresne II* (Hill and De Deckker, 2004; https://doi.org/10.17600/3200090). It was retrieved from a small plateau south of Kangaroo Island at 2420 m depth (36°43.80′S, 136°32.90′E) facing the mouth of the Murray River, between two conduits of the Du Couëdic Canyon (Fig. 1), and within the envelope of lower Circumpolar Deep Water and Indian Deep Water transported by the boundary current.

A detailed description of core MD03-2611 can be found in Hill and De Deckker (2004). The core has already been investigated for planktic foraminiferal assemblages (De Deckker et al., 2012, 2020; Moros et al., 2021), planktic (*Globigerina bulloides* and *Globigerinoides ruber*) stable isotope analysis (De Deckker et al., 2012, 2020), radiocarbon dating on planktic foraminifera (De Deckker et al., 2012, 2020), XRD and XRF analyses (De Deckker et al., 2012, 2020), alkenone palaeothermometry (De Deckker et al., 2020), and clay mineralogy (Gingele et al., 2004). Previous studies have demonstrated that core MD03-2611 is not impacted by processes of erosion and sediment redistribution, common phenomena in canyon systems but absent in core MD03-2611 since it was taken away from the main canyon conduit (Gingele et al., 2004; De Deckker et al., 2020). The core does not either demonstrate any hiatuses (Gingele et al., 2004; De Deckker et al., 2020; Moros et al., 2021), making it an ideal candidate to reconstruct surface-benthic interactions.

The chronology we use for the upper 910 cm of core MD03-2611 is constructed on 64 AMS ^{14}C planktic foraminifera dates previously published in Gingele et al. (2007), Moros et al. (2009, 2021), De Deckker et al. (2012, 2020), and Perner et al. (2018), and is an updated version of the latest chronology proposed by De Deckker et al. (2020) which used the Marine13 curve for age calibrations (Reimer et al., 2013) within the CALIB 7.0.2 software (Stuiver and Reimer, 1993). For this study, AMS ^{14}C dates were calibrated using the Marine20 calibration curve (Reimer et al., 2020), whilst the age model was constructed using Bayesian modelling with the *Rbacon* package for R (Blaauw and Christen, 2011). As suggested by De Deckker et al. (2020), we used a Delta R (local reservoir age) of 440 years throughout the Holocene back to 14 ^{14}C ka BP, and a Delta R of 600 and 700 years from 14 to 18 ^{14}C ka BP and older than 18 ^{14}C ka BP, respectively. Details of the age model are given in Supplementary Material 1. The chronology for the lower part of the core (from 910 to 1197 cm), which is out of the range of the AMS ^{14}C dating method, follows the age model constructed by De Deccker et al. (2020) which estimated ages by correlation with the adjacent core MD03-2607 (Fig. 1). The latter was dated by single-grain optically stimulated luminescence, combined with a correlation to the global δ^{18}O benthic stack of Lisiecki and Raymo (2005) (De Deckker et al., 2019). Further details are given in De Deckker et al. (2019). As demonstrated by its correlation to the benthic δ^{18}O stacks of Lisiecki and Raymo (2005) and Lisiecki and Raymo (2005) from offshore New Zealand, the core covers approximately the last 94 ka (i.e. from the end of Marine Isotope Stage - MIS 5c to the end of the Late Holocene). The correlation with the benthic δ^{18}O stack of Liesicki and Stern (2016) demonstrates that core MD03-2611 contains only little MIS 5c and MIS 5 b sediments, whereas MIS 5a is well recorded.

3.2. Benthic foraminiferal assemblage investigation

A total of 75 samples were taken from core MD03-2611, every 10 cm between the top of the core down to 4 m depth, and every 25 cm from 4 m to the bottom of the core (11.97 m depth), and examined for benthic foraminiferal assemblages (Supplementary Material 2). The samples were washed over a 63 μm mesh sieve, dried in an oven at 60 °C, and then split with a microsplitter. A minimum of 300 individuals were counted (Buzas, 1990; Fatela and Taborda, 2002) and picked from a single split, stored in plummer cells, and determined under the binocular microscope. Images of benthic foraminifera were taken using the Scanning Electron Microscope (SEM) at the Centre for Advanced Microscopy (Australian National University, Canberra) using the Zeiss UltraPlus analytical FESEM after gold coating the specimens in an EMITECH K550X coater. Group average hierarchical clustering was performed on all 75 samples using the Bray-Curtis similarity index on untransformed relative abundances of all identified species (%). This analysis separated two clusters which were then subjected to two separate group average hierarchical clustering, using the same approach as previously. Benthic foraminiferal species discriminating between clusters were identified by Similarity Percentage analyses (SIMPER). All hierarchical cluster and SIMPER analyses were performed using the PRIMER6 software (Clarke and Gorley, 2006). A detrended correspondence analysis (DCA) was carried out with the R software (*decorana* and *envfit* functions; R Team, 2022) on all samples using untransformed relative abundances of cluster discriminating species formerly identified by SIMPER analyses. The environmental vectors fitted to the ordination using the *envfit* function were the relative abundances of key planktic species (De Deckker et al., 2020), the planktic foraminiferal stable isotope records (De Deckker et al., 2020), the percentage of kaolinite, illite and smectite, together with the clay/silt ratio (Gingele et al., 2004), the weight percentage of quartz (obtained by XRD) and titanium counts (obtained by XRF scanning) (De Deckker et al., 2020), and the alkenone sea surface temperature (SST) record (De Deckker et al., 2020). All boxplots and graphs were created using the *ggplot2* package for R (Wickham, 2016).

4. Results

4.1. Benthic foraminiferal species distribution

A total of 429 benthic foraminifera species were identified within core MD03-2611, among which 23 are dominant and demonstrate relative abundances ≥5% (Supplementary Material 2). Over the full core length, the average 10 most abundant species (as percentages of the total foraminiferal counts) are *Gavelinopsis praegeri* (14.4%), *Rosalina vilardeboana* (6.7%), *Discorbinella araucana* (6.5%), *Bolivina variabilis* (6.4%), *Miliolinella subrotunda* (4%), *Globocassidulina* spp. (*Globocassidulina subglobosa* + *Globocassidulina canalisuturata*; 3.5%), *Cassidulina carinata* (2.7%), *Cibicides refulgens* (2.2%), *Rosalina paupereques* (2.1%), and *Elphidium crispum* (1.9%) (Fig. 2). Following the microhabitat preferences given by Hayward et al. (1997, 2010) and Murray (2006), 6 of these species are epibenthics (*G. praegeri*, *R. vilardeboana*, *D. araucana*, *M. subrotunda*, *C. refulgens*, and *R. paupereques*), whereas the 4 others are shallow infaunal (*B. variabilis*, *Globocassidulina* spp., *C. carinata*, and *E. crispum*) (Supplementary material 3). The total number of species per sample varies from 46 (475 cm depth) to 95 (5 cm depth), with an average value of 65 (Supplementary material 2). Shannon diversity ranges from 3.03 (1190 cm depth) to 3.92 (355 cm depth), with an average diversity of 3.47 (Supplementary material 2). MD03-2611 contains a number of benthic foraminifera which are characteristic of shallow-water/shelf environments (Li et al., 1996a; Hayward et al., 1999, 2010; Smith and Gallagher, 2003; Murray, 2006; Nash et al., 2018), and hence considered allochtonous at the core site. These species, noticeably belonging to the Ammoniidae, Elphidiidae, Glabratellidae, and Haynesinidae families, are referred to in the text as "shelf species". Their influence on the implemented statistical analyses was assessed by comparing the abundance of the main cluster-discriminating species when excluding or not the former from the analysed dataset. The comparison of abundances and the associated paired student t-tests show that the inclusion of shelf species does not change the observed trends in benthic foraminiferal distribution (Supplementary Material 4 and 5). All specimens throughout the core showed a relatively good preservation without any signs of dissolution, but with some visible borings and test damage (holes and etching; Fig. 2).

4.2. Benthic foraminiferal assemblage composition

The first group average hierarchical clustering performed on all 75 samples separated two clusters (A and B) at 45% similarity (Fig. 3a). Cluster A regroups 41 samples (MIS 1 and MIS 5a-c), and cluster B clumps all remaining 34 samples (MIS 4, 3 and 2) (Supplementary material 6). The 3 most abundant species in cluster A are *G. praegeri* (23.0% average abundance), *B. variabilis* (7.6% average abundance), and *R. vilardeboana* (5.3% average abundance), whilst *R. vilardeboana* (8.4% average abundance), *D. araucana* (8.0% average abundance), and *M. subrotunda* (6.0% average abundance) are the 3 most abundant species in cluster B (Fig. 2; Supplementary material 6). The most discriminating species between clusters A and B in of importance are *G. praegeri*, *D. araucana*, *R. vilardeboana*, *M. subrotunda*, *B. variabilis*, *R. paupereques*, *Miliolinella dilatata*, and *Globocassidulina* spp. (Figs. 2 and 3b). It is worthwhile to stress that *G. praegeri* contributes on its own to approximately 17% of the total dissimilarity between the two clusters, i.e. over 4 times more than the second most discriminating species *D. araucana* (Supplementary material 6).

Samples belonging to cluster A were submitted to a second group average hierarchical cluster analysis (Fig. 4a). Samples separated at 60.5% similarity between clusters c (20 samples), d (8 samples), e (11 samples), and 2 outliers (Fig. 4a). Cluster c is characterized by a greater abundance of *G. praegeri* (27.5% average abundance) and low abundances of *B. variabilis* (6.6% average abundance) and *C. refulgens* (2.0% average abundance) in comparison to clusters d and e (Fig. 4b), whilst the higher average abundances of *D. araucana* (7.4%) and *Globocassidulina minuta* (2.0%) together with the lower average abundances of *R. vilardeboana* (4.0%) and *Nuttalides umbonifera* (0.8%) typify cluster e (Figs. 2 and 4b; Supplementary material 7).

Likewise, a secondary group average hierarchical cluster analysis was carried out on samples from cluster B (Fig. 5a). Samples separated at 52% similarity between clusters f and g, excluding 8 outliers samples (Fig. 5a). With 7.2% against 1.8% average abundance, *G. praegeri* is noticeably more abundant in cluster f than cluster g (Fig. 5b). *Discorbinella araucana* shows an opposite trend with a higher average abundance within cluster g than f (9.9% against 5.9%; Fig. 5b). The infaunal *Globocassidulina* spp. and *C. carinata* are more abundant in cluster f (average abundances of 4.0% and 3.9%, respectively) than in cluster g (average abundances of 2.2% and 2.3%, respectively) (Fig. 2; Supplementary material 8). The shallow water-dwelling *Glabratella australensis* (Hayward et al., 1999; Murray, 2006), along with other shelf species, is more abundant in cluster g than f (Fig. 5b; Supplementary material 8).

4.3. Assemblage distribution and driving environmental variables

Cluster A corresponds to the Holocene and MIS 5a-c, whilst cluster B corresponds to the last glacial period (Fig. 6). Within cluster A, the periods from 93.3 to 76 ka and from 12.5 to 7.1 ka are characterized by cluster c (Fig. 6). These time intervals correspond to MIS 5a-c (Lisiecki and Raymo, 2005; Past Interglacials Working Group of PAGES, 2016) and most of the early Holocene as defined by Smith et al. (2011) and Reeves et al. (2013). An alternation between clusters d and e defines benthic foraminiferal assemblages during the last 7 ka, i.e. the mid and late Holocene (Fig. 6). During the last glacial period, cluster g is associated to MIS 2 (29–11.7 ka; Lisiecki and Raymo, 2005; Liesicki and Stern, 2016), whilst cluster f is essentially restricted to MIS 3 (59–29 ka; Lisiecki and Raymo, 2005; Liesicki and Stern, 2016; De Deckker et al., 2019) and the later stages of MIS 4 (71–59 ka; Lisiecki and Raymo, 2005; Liesicki and Stern, 2016; De Deckker et al., 2019). However, the 25 cm sampling interval combined to the reduced sedimentation rate makes it impossible to investigate MIS 4 benthic foraminiferal assemblages in detail.

High abundances of *G. praegeri* (associated with the Holocene and MIS 5a-c) show a positive correlation with warm SSTs and high abundances of the planktic *Globorotalia inflata* and *Globigerinoides ruber* (Fig. 7), whereas high abundances of miliolids and shelf species (associated with cluster B) demonstrate a positive correlation with low SSTs, high abundances of subpolar planktic foraminifera species, and high clay/silt, titanium, and quartz values (Fig. 7). *Discorbinella araucana*, *R. vilardeboana* and *R. paupereques*, associated with the last glacial period, show positive correlations with high abundances of *Globorotalia truncatulinoides* and *G. bulloides* (Fig. 7).

5. Discussion

5.1. Influence of terrestrial input on deep-sea benthic ecosystems

The abundance of shallow-water dwelling foraminifera species, essentially belonging to the Ammoniidae, Elphidiidae, Glabratellidae, and Haynesinidae families, points to a transport of these benthic foraminifera from proximal settings (Fig. 6). All the aforementioned foraminiferal families are small, epifaunal, overall flat-shaped organisms, and are consequently prone to transport in suspension by currents and river plumes (Duros et al., 2012; Garcia et al., 2013; Mojtahid et al., 2013, 2020). *Rosalina vilardeboana* and *R. paupereques* are presumably also allochtonous at the core site, as rosalinids are reported as shelf dwellers, despite rare lower-bathyal occurrences of some species probably resulting from their displacement (Hayward et al., 1999, 2010; Debenay, 2012). *Rosalina* spp. is known to attach to seaweed along the coastline and within shallow bays and lagoons, and can then float out to sea when its substrate is displaced by currents (Spindler, 1980; Hayward

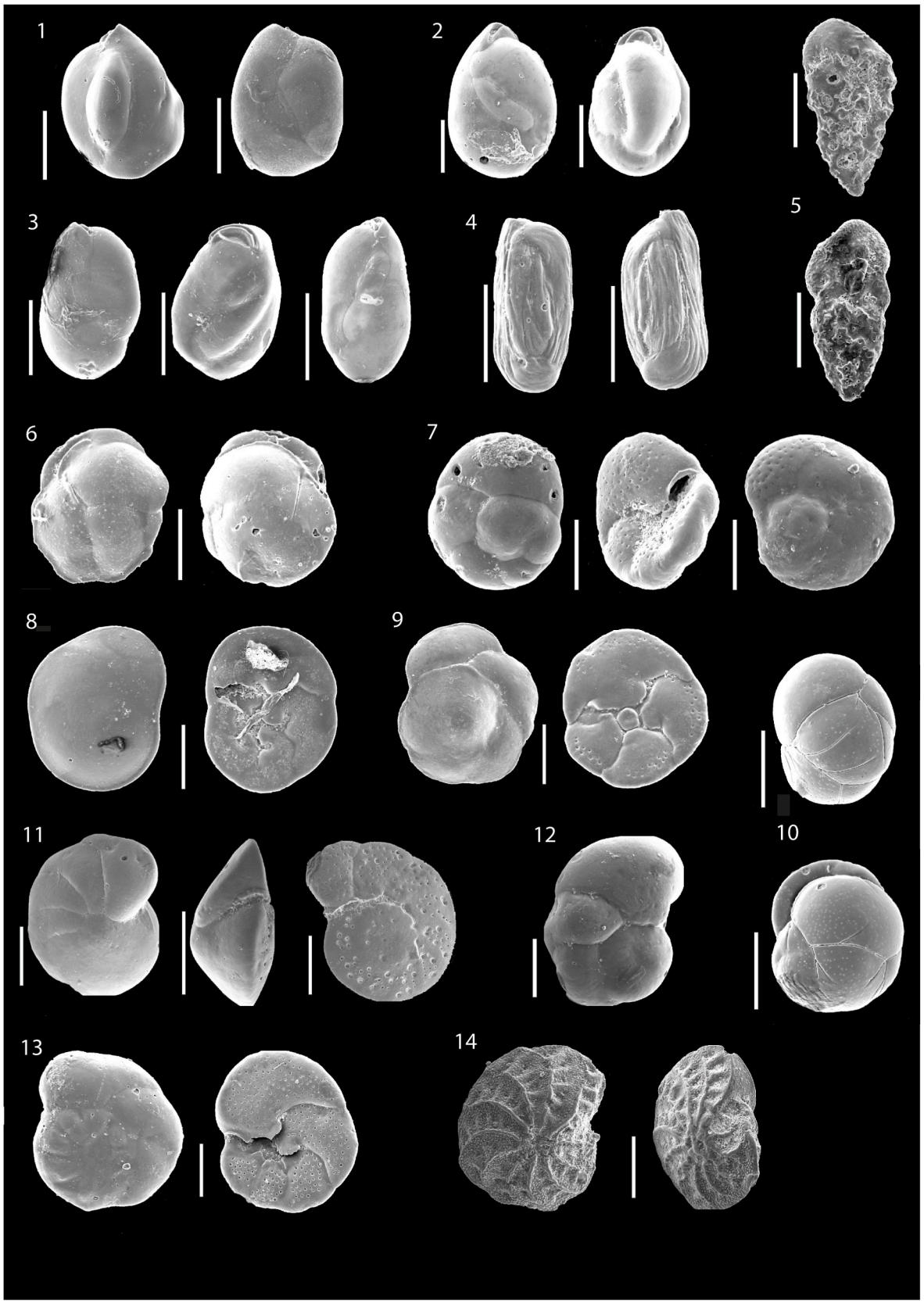

Fig. 2. Scanning Electron Microscopy images of common foraminifera in core MD03-2611.**1**. *Miliolinella dilatata* (d'Orbigny, 1839); **2**. *Miliolinella subrotunda* (Montagu, 1803); **3**. *Miliolinella elongata* (Kruit, 1955); **4**. *Quinqueloculina delicatula* (Vella, 1957); **5**. *Bolivina variabilis* (Williamson, 1858); **6**. *Cassidulina carinata* (Silvestri, 1896); **7**. *Rosalina vilardeboana* (d'Orbigny, 1839); **8**. *Rosalina paupereques* (Vella, 1957); **9**. *Gavelinopsis praegeri* (Heron-Allen & Earland, 1913); **10**. *Globocassidulina subglobosa* (Brady, 1881); **11**. *Cibicides refulgens* (Montfort, 1808); **12**. *Cibicides lobatulus* (Walker & Jacob, 1798); **13**. *Discorbinella araucana* (d'Orbigny, 1839); **14**. *Elphidium macellum* (Fichtel & Moll, 1798). All scale bars represent 100 μm.

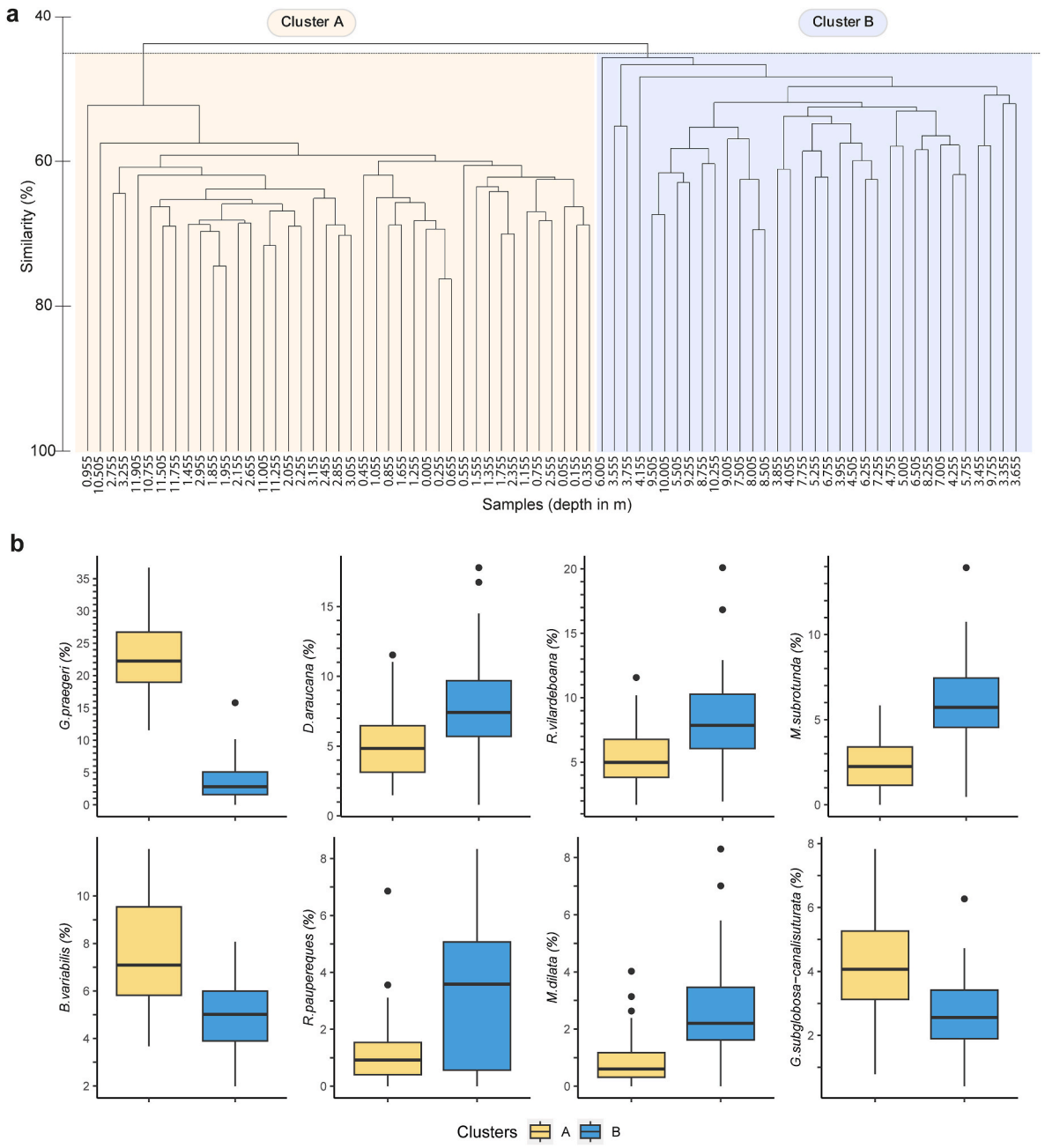

Fig. 3. **a**) Hierarchical cluster analysis (group average) performed on relative abundances (%) of benthic foraminiferal assemblages from all 75 samples (from core MD03-2611) using Bray-Curtis similarity index on untransformed data. Clusters A (yellow) and B (blue) separate at 45% similarity. **b**) Boxplots illustrating the relative abundances (%) of the 8 most discriminating benthic foraminifera species (names on vertical axis) between clusters A and B determined by Similarity Percentage analysis (Supplementary Material 6).

et al., 1999; Murray, 2006). Not much is known about the ecology of *D. araucana*, which is common during glacial periods at the core site (Figs. 3 and 6), though its flat trochospiral morphology and its North Atlantic distribution (Corliss and Chen, 1988; Koho et al., 2008) led Bunzel et al. (2017) to classify it as an epibenthic species within MIS 5 fossil assemblages found at approximately 380 m water depth in the Inner Sea of the Maldives. The related *D. bertheloti* prefers oxic conditions at depths between 30 and 600 m off the coasts of Southeast Australia and New Zealand (Smith and Gallagher, 2003; Hayward et al., 2010). Thus, in the same way as rosalinids, *D. araucana* is quite possibly subject to downslope transport and may be considered allochtonous at 2420 m depth, though the scarcity of knowledge concerning the ecology of this species only allows a tentative interpretation. Some miliolids, particularly *Quinqueloculina* spp., are documented to inhabit the shallow parts of the Bass Canyon off South Australia (Smith and Gallagher, 2003). Representatives of this genus are thus possibly also transported to the core site from the shelf. Mojtahid et al. (2020) described a similar association of shallow-water benthic foraminifera composed of Elphidiidae, Haynesinidae and Rosalinidae from core SS02/06-GC2 retrieved at 5078 m depth south of the upper Sprigg Canyon Group (Fig. 1b). Based on the observed sedimentary sequences, these authors proposed that shelf-dwelling foraminiferal communities were transported to bathyal and abyssal depths by gravity flows triggered by discharges from the River Murray. These authors added that shelf species are mostly transported via meso/hypopycnal flows and deposited by hemipelagic sedimentation, whereas bathyal species would be transported by

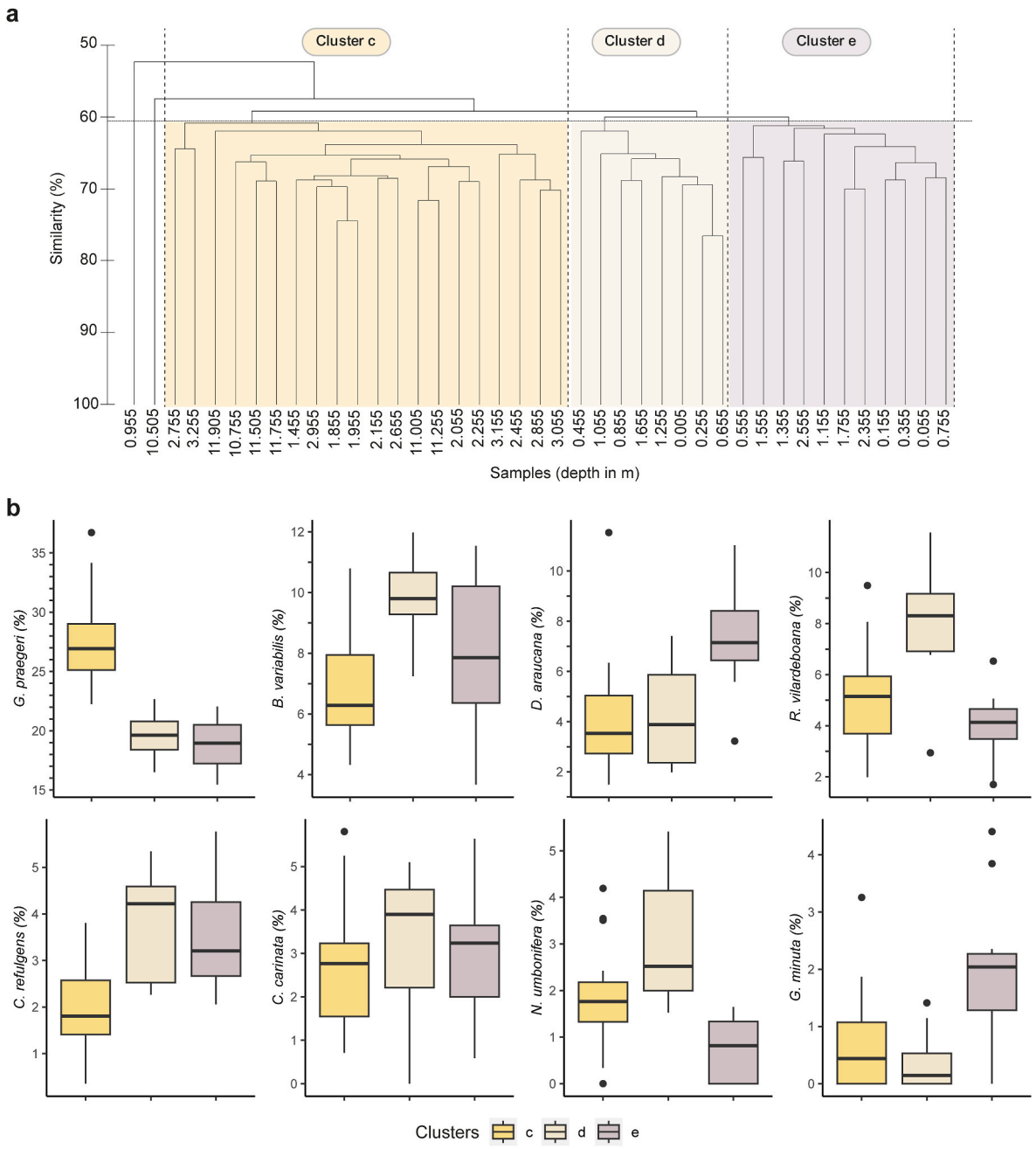

Fig. 4. **a**) Hierarchical cluster analysis (group average) performed on relative abundances (%) of benthic foraminiferal assemblages from samples belonging to Cluster A (see Fig. 3) using Bray-Curtis similarity index on untransformed data. Clusters c, d, and e separate at 60.5% similarity. **b**) Boxplots illustrating the relative abundances (%) of the 8 most discriminating benthic foraminifera species (names on vertical axis) between clusters c, d, and e determined by Similarity Percentage analysis (Supplementary Material 7).

hyperpycnal flows and bedload transport (Mojtahid et al., 2020). In contrast to core SS02/06-GC2, neither signs of sediment redistribution, nor erosive contacts, nor Bouma-type sequences are observed in core MD03-2611 (Hill and De Deckker, 2004). This implies that turbidite deposits are absent within core MD03-2611 and that deep-dwelling benthic communities can be considered in situ and being unaffected by hyperpycnal flows. As suggested by Gingele et al. (2004), we utilize the clay/silt ratio as a proxy for the input of river suspension versus aeolian dust, as the suspended load of rivers in the area is predominantly situated in the clay-size range and that aeolian dust is in contrast rather in the silt range (Woodyer, 1978; Hesse and McTainsh, 1999). The clay/silt ratio shows a positive correlation with shelf species, with joint high values during glacial periods and maximum values during the LGM (Figs. 7 and 8). Given the current shallowness of the Lacepede Shelf, the lower sea-level during MIS 2 reduced the distance between the River Murray mouth and the core site to approximately 50 km (Figs. 1 and 9). Hypo/mesopycnal flows prompted by fluvial discharges would have displaced benthic foraminifera inhabiting the shelf and eventually deposited them within deep-sea environments (Fig. 9). The presence of closed ostracod valves and other shallow water organisms in the core (e.g. octocorals) confirms that allochtonous carbonate material reached the core site (Gingele and De Deckker, 2005). Given the distribution of shelf-dwelling benthic foraminifera species during MIS 2, with relative abundances fluctuating from 4 to 16%, it is apparent that discharges from the River Murray and associated hypo/mesopycnal flows were intermittent (Fig. 8). Conversely, sea-level rise during warmer periods

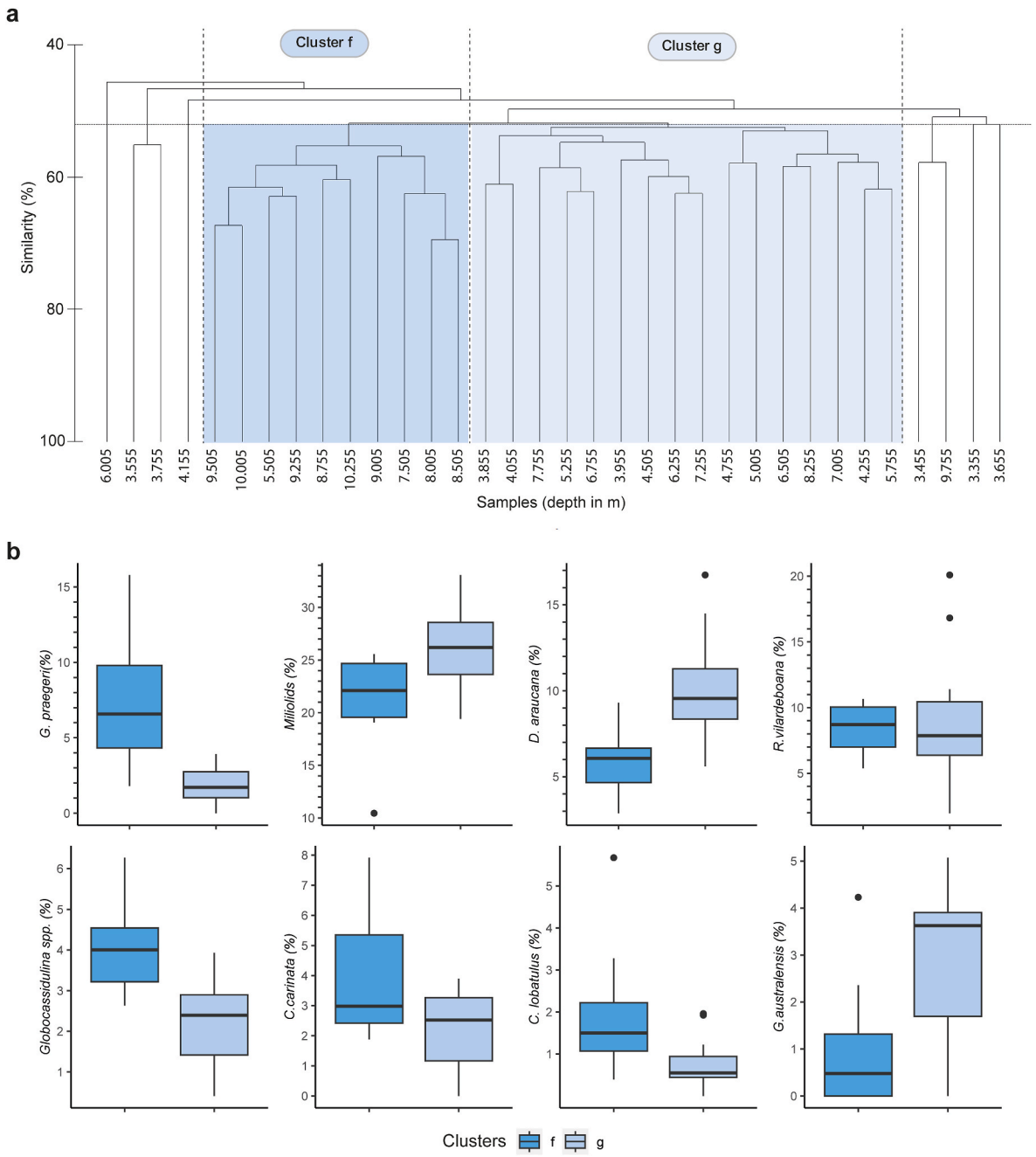

Fig. 5. **a**) Hierarchical cluster analysis (group average) performed on relative abundances (%) of benthic foraminiferal assemblages from samples belonging to Cluster B (see Fig. 3) using Bray-Curtis similarity index on untransformed data. Clusters f and g separate at 52% similarity. **b**) Boxplots illustrating the relative abundance (%) of the 8 most discriminating benthic foraminifera species (names on vertical axis) between clusters f and g determined by Similarity Percentage analysis (Supplementary Material 8).

would have considerably reduced the arrival of allochtonous foraminifera within deep-sea habitats (Figs. 8 and 9).

If hypo/mesopycnal flows sparked the transport of abundant shelf species to the deep-sea, it is not evident that these episodes were associated with an increased export of organic matter to the seafloor. Indeed, based on Total Organic Carbon concentrations and paleoproductivity estimates, Gingele and De Deckker (2005) demonstrated that the supply of nutrients from the River Murray insignificantly affected paleoproductivity during the last 150 ka. This observation is confirmed by the composition of benthic foraminiferal assemblages during the last 94 ka. Assemblages observed during periods marked by high clay/silt ratios and high numbers of shelf species, such as MIS 2, are characterized by high abundances of miliolids (Figs. 3 and 6–8). Indeed, miliolids show a clear preference for cold periods, as evidenced by the negative correlation between their relative abundance and alkenone-derived SST values throughout the core, although their relative abundance shows little variability between MIS 5a-c and early MIS 4, and MIS 4 and MIS 2 (Figs. 7 and 8). Modern and fossil foraminiferal communities dominated by miliolids, such as the predominant species found at the study site (*M. subrotunda*, *M. dilatata*, *Quinqueloculina* spp., *Pyrgo* spp.), are associated to oxic conditions within oligotrophic to mesotrophic environments (Mullineaux and Lohmann, 1981; Schmiedl et al., 2003; Smith and Gallagher, 2003; Murray, 2006). Hence, the abundance of miliolids during cold glacial periods (Cluster B) suggests that the deep benthic environments were well ventilated and oligotrophic (Figs. 3, 6 and 7). Conversely, warm climate periods (Cluster A) are characterized by lower

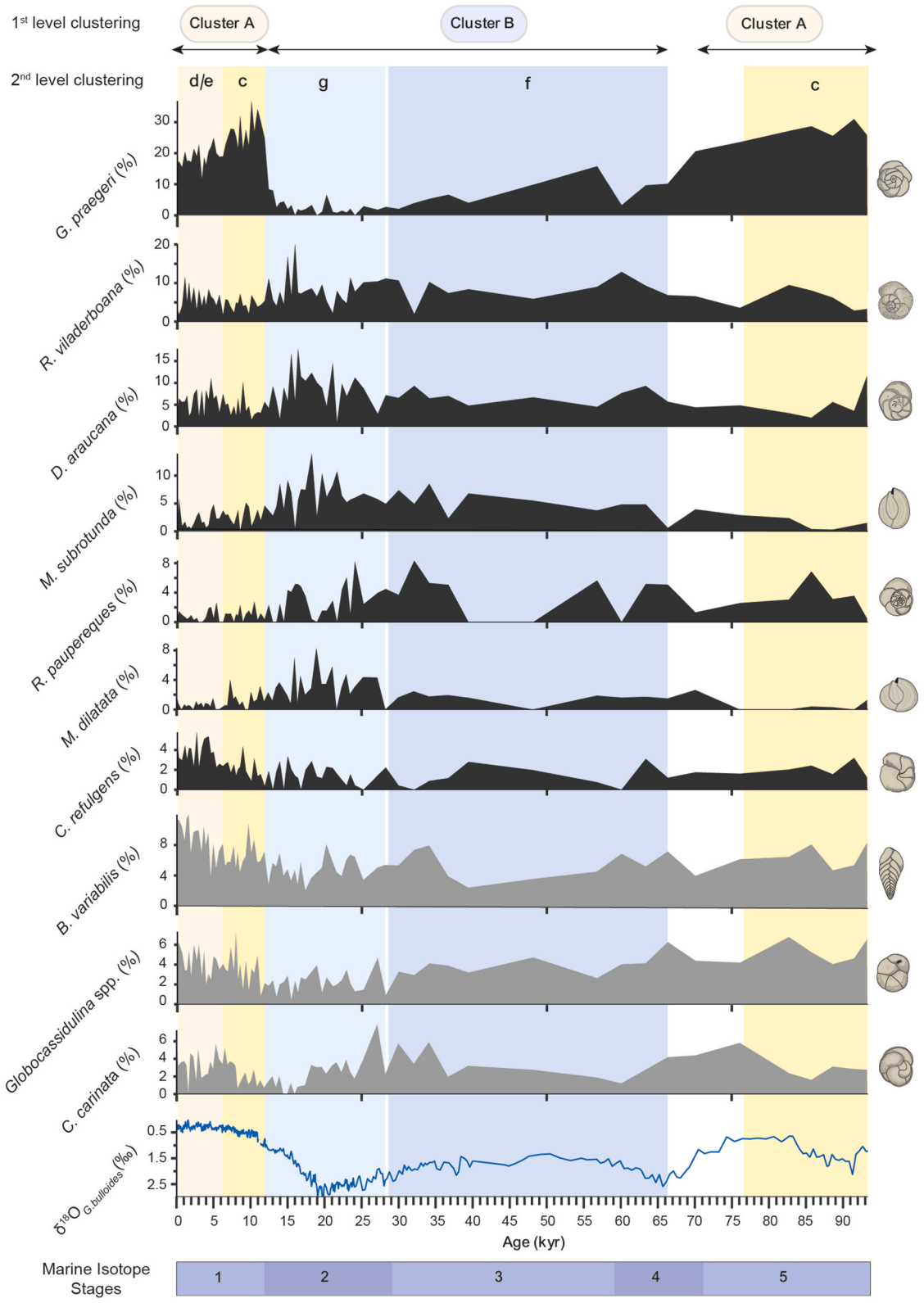

Fig. 6. Distribution of dominant benthic foraminiferal species (relative abundance >5%, this study) and $\delta^{18}O$ record of the planktonic foraminifera *G. bulloides* in core MD03-2611 (De Deckker et al., 2020). The different clusters are indicated together with the Marine Isotope Stages (following Lisiecki and Raymo, 2005; Liesicki and Stern, 2016; De Deckker et al., 2019). The limits of clusters A and B are given by the arrows at the top of the figure, whilst the boundaries of clusters c, d/e, f, and g are indicated by the shaded coloured areas (pale yellow: clusters d/e; bright yellow: cluster c; light blue: cluster g; dark blue: cluster f; white: no 2nd level clustering). The colour code of clusters follows those of Figs. 3–5. Grey and black curves correspond respectively to infaunal and epifaunal species. Note the Marine Isotopic Stages defined at the bottom of the figure.

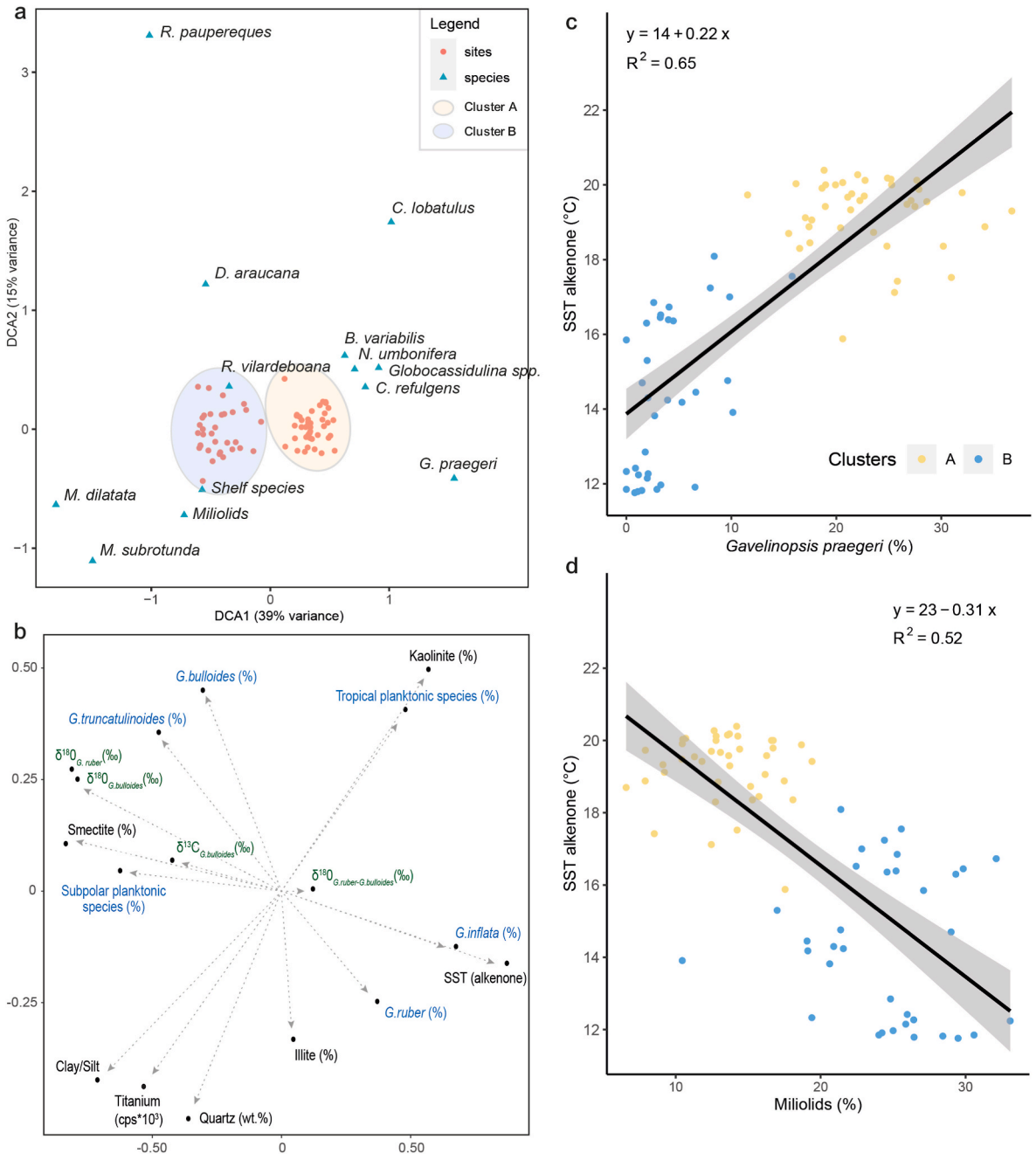

Fig. 7. **a**) Detrended correspondence analysis (DCA) performed on untransformed benthic foraminiferal assemblage data (relative abundances) from core MD03-2611. Only discriminating species identified using the Similarity Percentage analysis are integrated to the analysis. Clusters A and B (defined by hierarchical cluster analysis, see Fig. 3) are overlaid. **b**) Environmental vectors explaining the observed foraminiferal and sample ordination as observed in **a** (data from Gingele et al., 2004, De Deckker et al., 2020; Moros et al., 2021). Blue and green fonts indicate key planktic foraminifera species and stable isotope records of planktic foraminifera, respectively. **c**) Relationship between the relative abundance (%) of the benthic species *G. praegeri* and Sea Surface Temperature (°C) obtained by alkenometry (see text). **d**) Relationship between the relative abundance (%) of miliolids and Sea Surface Temperature (°C). In both c and d, yellow and blue dots correspond to clusters A and B (see Fig. 3), respectively.

numbers of miliolids and a greater abundance of infaunal species, noticeably *B. variabilis* and *Globocassidulina* spp. (Figs. 3 and 6–8). *Globocassidulina* spp. is regularly found after pulses of phytodetritus deposition, whereas *B. variabilis* is rather associated to continuous and high fluxes of organic carbon input and reduced seafloor oxygenation (Gooday, 1993; De Rijk et al., 2000; Suhr et al., 2003; Smart et al., 2010; Dias et al., 2018). The association of these species, together with the relative scarcity of miliolids, points to an overall reduced oxygenation associated to organic matter input during MIS 5a-c and the Holocene. Within the latter, greater organic matter input and weaker seafloor oxygenation would have been accentuated during the mid and late Holocene, as evidenced by the higher abundance of *B. variabilis* as shown by Clusters d and e compared to Cluster c (Fig. 4). This confirms the observations made by Nees et al. (1999), which noticed a similar increase in productivity-indicator benthic foraminiferal species during the Holocene at 2260 m depth on the South Tasman Rise.

In contrast with the River Murray's discharges, there is evidence that dust was predominantly brought by strong westerly winds from the Australian central deserts during cold and dry periods, noticeably during MIS 2 and 4 as evidenced by high Ti total counts and $\delta^{13}C_{G.bulloides}$ values

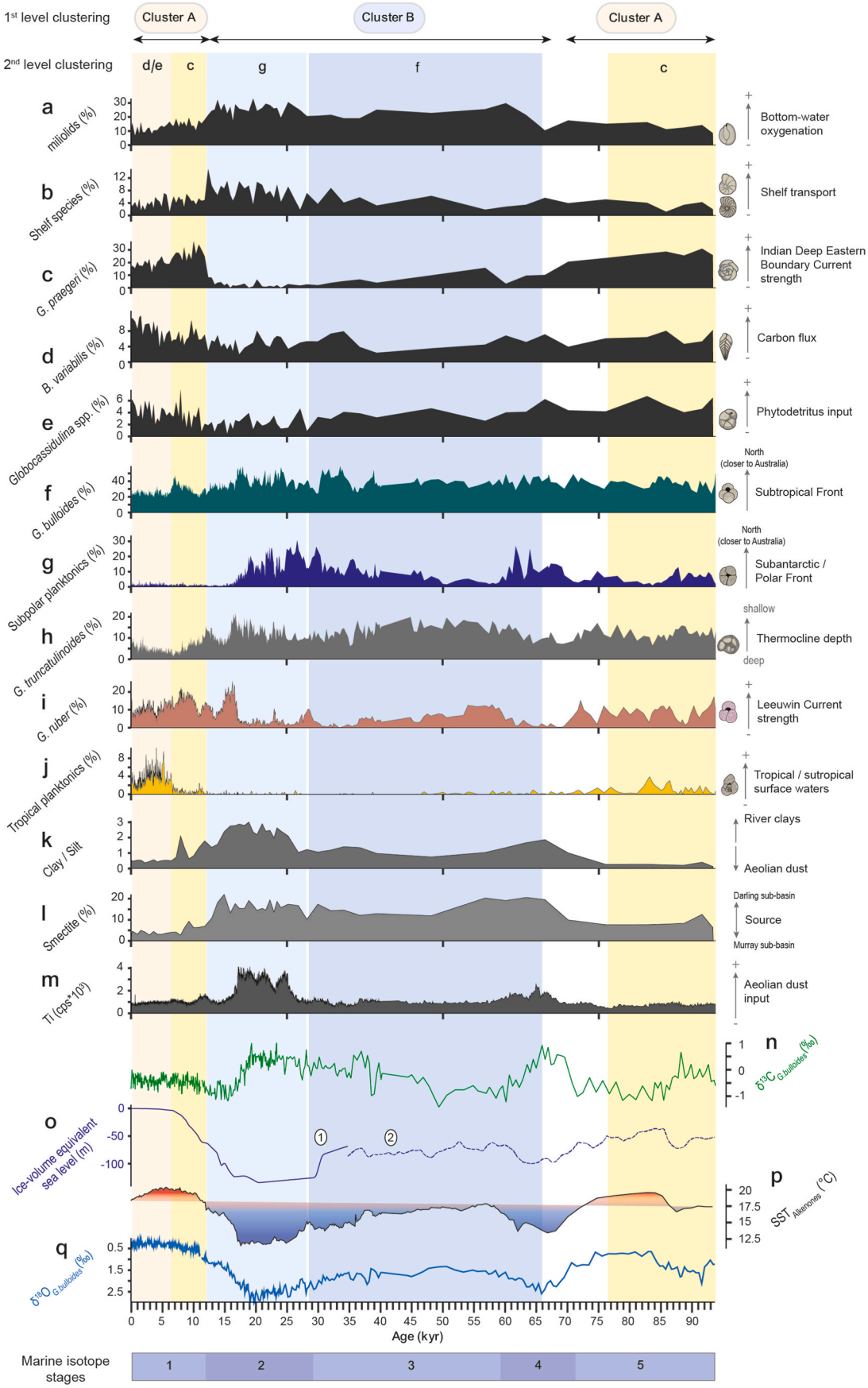

(caption on next page)

Fig. 8. Distribution of selected proxies for core MD03-2611. The different clusters are indicated together with the Marine Isotope Stages (following Lisiecki and Raymo, 2005; De Deckker et al., 2019). The limits of clusters A and B, and c, d/e, f, and g are respectively indicated by the arrows and shaded areas (see caption Fig. 6 for details). **a**) relative abundance of all miliolids used as an indicator for seafloor oxygenation, **b**) relative abundance of allochtonous benthic foraminiferal shelf species, **c**) relative abundance of the epibenthic *G. praegeri*, **d**) relative abundance of the infaunal high carbon flux indicator *B. variabilis*, **e**) relative abundance of the infaunal phytodetritus feeder *Globocassidulina* spp. (*G. subglobosa* + *G. canalisuturata*), **f**) relative abundance of the planktic foraminifera *G. bulloides*, an indicator of Subtropical Front proximity to Australia (De Deckker et al., 2020), **g**) relative abundance of subpolar planktic foraminifera species (*N. pachyderma* and *T. quinqueloba*; De Deckker et al., 2020), **h**) relative abundance of the deep-water dwelling planktic foraminifera *G. truncatulinoides* (De Deckker et al., 2020), **i**) relative abundance of the subtropical planktic foraminifera *G. ruber*, an indicator of the presence of the Leeuwin Current offshore South Australia (De Deckker et al., 2020), **j**) relative abundance of tropical planktic foraminifera species (*G. rubescens* + *G. tenella*; Perner et al., 2018; De Deckker et al., 2020); **k**) clay/silt ratio used to identify periods of dominant river vs. aeolian influence (Gingele et al., 2004), **l**) percentage of smectite (Gingele et al., 2004) used as an indicator of sub-basin source, **m**) total counts per second (cps.10^3) of titanium (De Deckker et al., 2012, 2020), **n**) $\delta^{13}C$ record of the planktic *G. bulloides* (De Deckker et al., 2020), **o**) relative sea-level; the period from 0 to 35 ka (1, full line) is based on Lambeck et al. (2014), whereas the period from 35 to 93 ka (2, dashed line) uses the data of Grant et al. (2012) **p**) mean annual alkenometry Sea Surface Temperature (SST) record obtained by alkenometry (De Deckker et al., 2020). Shaded red and blue colours respectively indicate relatively warm and cold conditions compared to today, **q**) $\delta^{18}O$ record of the planktic *G. bulloides*, being a proxy for sea level position (De Deckker et al., 2020).

(Figs. 8 and 9) that resulted in increased paleoproductivity (Gingele and De Deckker, 2005; De Deckker et al., 2020). Yet, benthic foraminiferal assemblages from the deep-sea do not seem to respond to these changes in aeolian dust import and the subsequent surface water productivity shifts. Indeed, as a high carbon flux-indicator species, the lower abundance of *B. variabilis* during glacial periods does not corroborate the documented, dust-driven surface productivity increase (Fig. 8). This observation is supported by the high abundance of miliolids during periods characterized by elevated aeolian dust input, suggesting that benthic conditions were oligotrophic. Organic carbon derived from aeolian dust input would either not have reached the seafloor, or would have been insignificant compared to the contribution of laterally-sourced organic carbon (Fig. 8). Thus, besides the greater transport of allochtonous shelf species during glacial periods, and in particular during the LGM, terrestrial input (i.e. aeolian dust and river discharges) does not appear to steer the distribution and variability of deep-sea-dwelling benthic communities at site MD03-2611 during the last 94 ka. This highlights that changes in the deep-sea and continental realms are overall decoupled during this considered time interval. Other environmental drivers, such as the influence of shifting surface and benthic currents throughout the last 94 ka, need also to be considered.

5.2. Benthic current variability during the last 94 ka

In addition to the high abundance of the infaunal *B. variabilis* and *G. subglobosa*, the Holocene and MIS 5a-c are characterized by significant numbers of the small epibenthic *G. praegeri* which show a clear correlation with high alkenone-derived SST values (Figs. 3 and 7). This species has been observed living within mid-bathyal environments between 500 and 1000 m depth at the Campbell Plateau off the southern coast of New Zealand (Hayward et al., 2007, 2013), and off the coast of Portugal and of eastern Brazil, respectively at 1450–2100 and 950–1250 m depth intervals (Seiler, 1975; Saupe et al., 2022). It has also been observed down to 2000 m in the open Northeast Atlantic (Weston, 1982), and is characteristic of assemblages in the Porcupine Seabight-Whittard Canyon area (Northeast Atlantic; Weston, 1985) and on the Australian-Irian Jaya continental margin (eastern Indonesia; Van Marle, 1988), respectively, at depth ranges between 1350-1600 m and 400–1500 m. It is otherwise confined to shallower sites across the world's oceanic shelves (Murray, 1970, 2006; Barmawidjaja et al., 1995; De Stigter et al., 1996; Altenbach et al., 2003; Saidova, 2008; Hayward et al., 2010). The abundance of *G. praegeri* at 2420 m depth off the southern coast of Australia is therefore one of the deepest fossil occurrences of this species, and contrasts with assemblages described from similar depths along New Zealand and in the southeast Indian Ocean (Corliss, 1979; Peterson, 1984; Murgese and De Deckker, 2005; Hayward et al., 2010). The possibility that such high numbers of well-preserved *G. praegeri* specimens were transported downslope from shallower settings may be dismissed given that it is the most abundant during warm periods when allochtonous shelf species are scarce, and that the River Murray mouth was situated far from the core site (Figs. 8 and 9).

Gavelinopsis praegeri attaches itself to hard substrates and is described as a passive suspension feeder preferring a sustained moderate food flux under dynamic bottom-current regimes (Murray, 2006; Hayward et al., 2010, 2013; Martins et al., 2015; Fentimen et al., 2020). Deep-sea settings are dynamic and affected by bottom currents driven by winds, tides or by the thermohaline circulation (Stow and Smillie, 2020 and references therein). Currents formed along continental margins and the abyssal plain may transport sediment matter along-slope, whilst also shaping the morphology of deep-sea habitats (Stow, 1982; Rebesco et al., 2014; Stow et al., 2019). Moreover, seafloor topographic features (e.g. ridges, gateways, canyons) may speed-up bottom currents, especially when slopes are steep or when gateways are narrow (Stow et al., 2019). Bottom-current intensity can enhance the amount of organic matter that is re-suspended, deposited or directly provided by the hemipelagic rain (Thomsen et al., 2002; McCave, 2008; Miguez-Salas et al., 2020). We suggest that the benthic foraminiferal assemblage associated to warm periods, noticeably the predominance of *G. praegeri*, *G. subglobosa* and *B. variabilis*, together with the higher abundance of the epibenthic *C. lobatulus* and *C. refulgens* in comparison to glacial periods (Fig. 7), translates to a strengthening of bottom currents and a funnelling of re-suspended particulate organic matter within the Murray Canyons which would provide food for foraminiferal communities (Fig. 9). This hypothesis is supported by the study of Tamsitt et al. (2019) whom, thanks to a combination of hydrographic measurements and Lagrangian experiments, evidenced the existence of a deep boundary current flowing eastward along South Australia between 1500 and 3000 m depth (Fig. 1a). A North-South oriented hydrographic section situated at 132°E showed that zonal velocity is the highest (±0.028 m s^{-1}) between approximately 1500 and 2500 m depth off the coast of South Australia (Tamsitt et al., 2019). In contrast to zonal velocity, oxygen concentration is the lowest (170–180 μmol kg^{-1}) between approximately 1500 and 2500 m depth off the coast of South Australia (Tamsitt et al., 2019). In addition, two North-South oriented hydrographic sections located at Cape Leeuwin and south of Tasmania indicate that total dissolved inorganic carbon is the highest (1160–2270 μmol kg^{-1}) near the continental margin between 2000 and 3000 m (Tamsitt et al., 2019). Tamsitt et al. (2019) suggested that these comparatively low-oxygen and carbon-rich waters were transported by the deep eastern boundary current and matched the properties of Indian Deep Water. It may be hypothesized that the Holocene and MIS 5a-c benthic foraminiferal assemblages, noticeably the abundance of *B. variabilis* and *Globocassidulina* spp., together with a relative scarcity of miliolids (Figs. 8 and 9), reflect this influence of comparatively low-oxygen and carbon-rich Indian Deep Water. In addition to the funnelling of re-suspended particulate organic matter, dissolved inorganic carbon could possibly be consumed by archaea and bacteria situated in the bathypelagic zone (i.e. between 1000 and 4000 m depth; Arístegui et al., 2009), providing an additional food source for foraminiferal communities. Further investigations would be

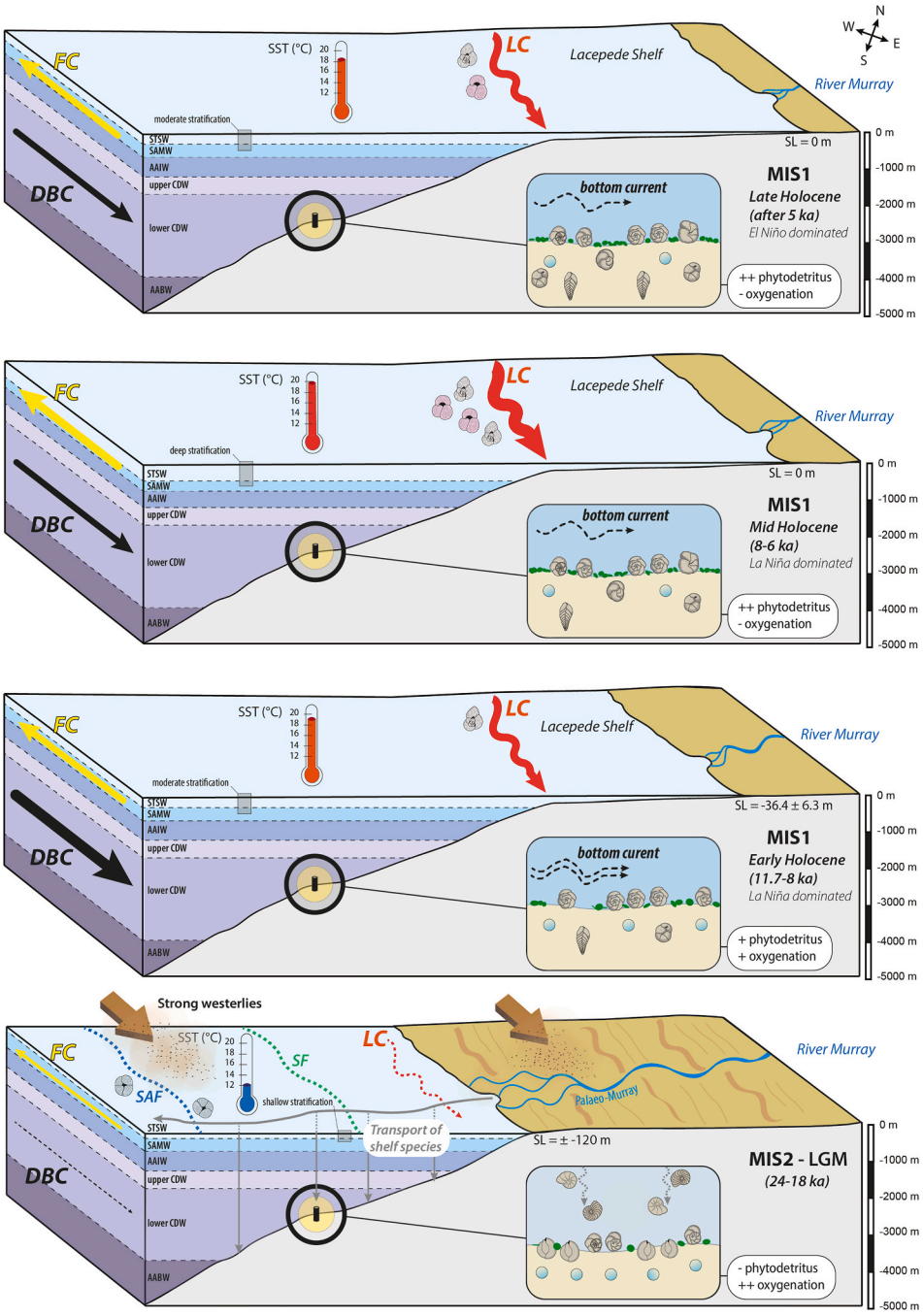

Fig. 9. Schematic diagrams illustrating the benthic and pelagic compartments and their dynamics at site MD03-2611 (black circles, close-up of the seafloor in the rectangle to the right) during key intervals of the last 94 ka. The Sea Surface Temperature (SST) values follow the alkenone palaeothermometry of De Deckker et al. (2020), whilst the relative sea level (SL) and extent of the Lacepede Shelf are indicated according to Lambeck et al. (2014) (25–0 ka) and Grant et al. (2012) (93–35 ka). The varying thickness of arrows indicates the strength of the Leeuwin Current (LC), Flinders Current (FC) and Indian Deep Eastern Boundary Current (DBC), based on planktic and benthic foraminiferal assemblage data (De Deckker et al., 2020; Moros et al., 2021; this study). Subtropical Front (SF) and Subantarctic Front (SAF) positions are given according to De Deckker et al. (2020) and Moros et al. (2021). The water mass boundaries are given according to James and Bone (2011) for Subtropical Surface Water (STSW), Subantarctic Mode Water (SAMW), and Antarctic Intermediate Water (AAIW); and according to Passlow et al. (1997) for Circumpolar Deep Water (CDW) and Antarctic Bottom Water (AABW). Trends of the El Niño-Southern Oscillation during the Holocene are given according to Moros et al. (2009) and Perner et al. (2018). The illustrated planktic and benthic foraminifera do not intend to encompass the full species diversity but are rather intended to stress changes amongst key species from one time interval to another. The barchans-type dunes during MIS 3 indicate a decrease in the westerlies compared to the LGM when the Lacepede Shelf was covered by transverse dunes.

needed to thoroughly document the widespread impact of the deep eastern boundary current on deep-sea environments along the South Australian margin.

5.3. Relationship between planktic and benthic domains

The composition of the glacial benthic foraminiferal assemblage (Cluster B; Fig. 3) implies a weakening of bottom currents and a reduced

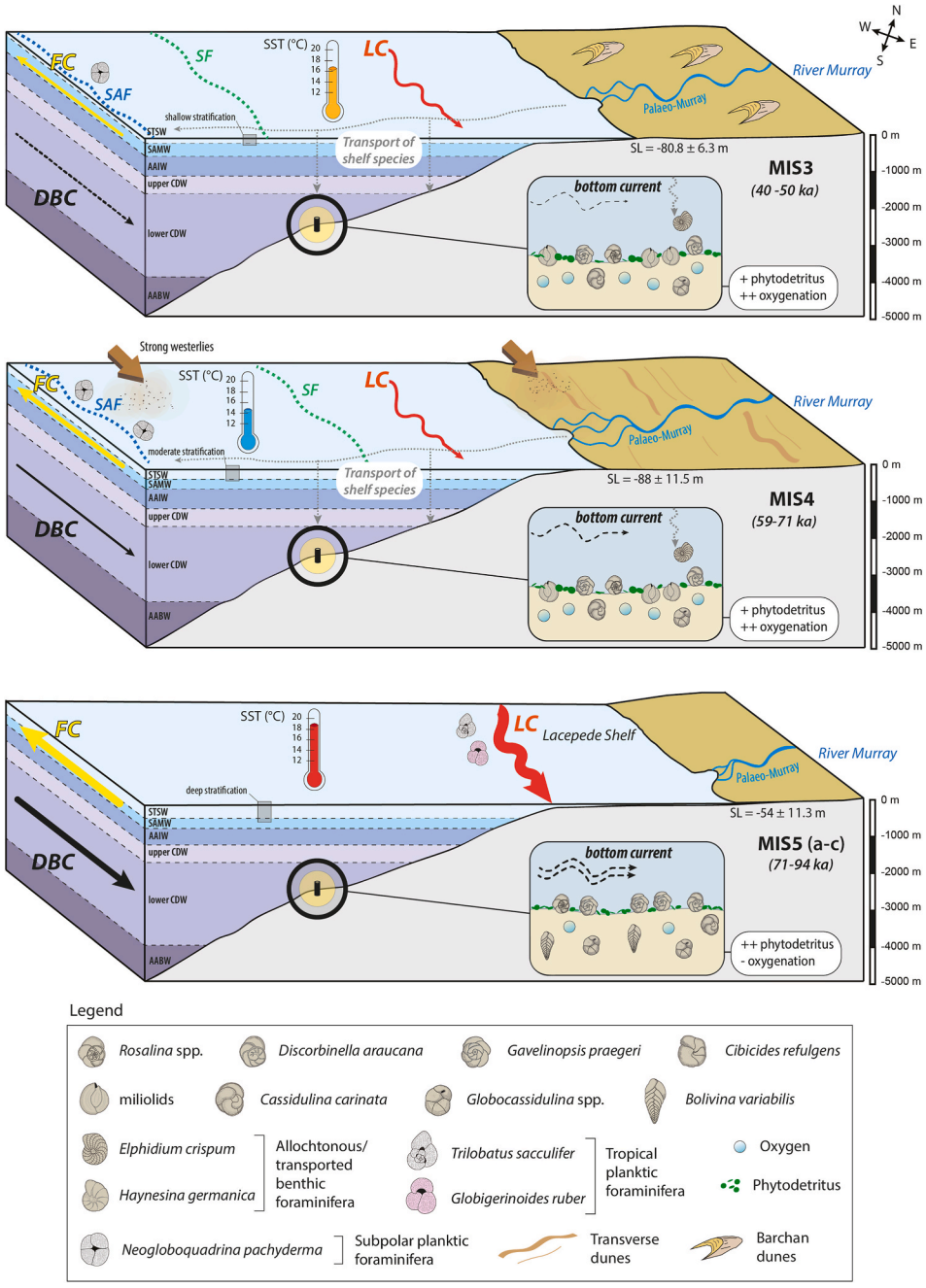

Fig. 9. (*continued*).

arrival of organic matter to the seafloor, possibly linked to a dwindling of the deep eastern boundary current. Within the last glacial period, the lower abundances of *G. praegeri* and *G. subglobosa* in cluster g (Figs. 5 and 6) would indicate that the deep eastern boundary current was the weakest during MIS 2 and rapidly picked up at the dawn of the last termination (Fig. 9). In addition, oxygen-rich waters must have bathed the core site during glacial periods and favoured the development of miliolids (Figs. 8 and 9). During the last glacial period, noticeably during the LGM, the Subtropical and Subantarctic fronts were located more northward, close to the South Australian coast, as a result of a stronger or more northward situated westerlies belt, as evidenced by high abundances of *Neogloboquadrina pachyderma* and *G. bulloides* (Figs. 8 and 9; De Deckker et al., 2020). In contrast, the LC would have been absent or severely reduced (Figs. 8 and 9; De Deckker et al., 2020). The northward migration of the Subtropical and Subantarctic fronts, as recorded by planktic foraminifera, coincides with changes in benthic foraminiferal assemblages, and the clear relationship between the two most assemblage-discriminating species (miliolids and *G. praegeri*) and alkenone-derived sea surface temperatures (Figs. 7–9). These observations indicate that the position and make up of deep-waters shifted following a similar time frame as the documented northward displacement of the Subtropical and Subantarctic fronts. We propose that oxygen-rich and oligotrophic conditions at the seafloor during glacial periods could reflect a stronger influence of oxygen-rich AABW at the core site and a greater stratification of the water column. The shoaling of this deep water mass and its mixing with overlying oxygen-poor

Circumpolar Deep Water would have changed the water composition at the core site, increasing dissolved oxygen content and reducing nutrient availability, thus triggering a shift in benthic communities (Figs. 3 and 6). The shoaling of AABW would have coincided with the northward displacement of the Subtropical and Subantarctic fronts (Figs. 8 and 9).

The southward retreat of the Subtropical and Subantarctic fronts during terminations as evidenced by the high abundances of *G. ruber* and *G. inflata*, noticeably between ~22 to 18.5 ka, coincided with a strengthening of the LC, which transports tropical warm waters along the South Australian margin (Figs. 8 and 9; De Deckker et al., 2020; Moros et al., 2021). This poleward displacement of these oceanic fronts is also seen in West and East Antarctica ice cores (Grootes et al., 1993). The presence of tropical planktic foraminifera (*Globoturborotalita rubescens* and *Globigerinoides tenella*), indicating the presence of tropical/subtropical waters originating from the Indo-Pacific Warm Pool above the core site (Perner et al., 2018), coincides with the change from cluster B to A (Fig. 8). Likewise, the increase in abundance of tropical planktic foraminifera during the Holocene mirrors the shift from assemblage c to d/e (Fig. 8). Assemblages d/e are both characterized by a greater abundance of *B. variabilis* and of the epibenthic *C. refulgens* (Fig. 4). *C. refulgens* lives attached to stable surfaces, using different feeding strategies in dynamic environments with variable food supply (Alexander and DeLaca, 1987; Schönfeld, 1997; Fentimen et al., 2021). Bearing in mind that the separation between assemblages c and d/e occurs at a relative high similarity and that interpretations are hence tentative, the mid and late Holocene appear to be marked by a more continuous flux of organic matter to the seafloor than the early Holocene, whilst bottom currents would have remained dynamic.

The strength of the LC appears to have peaked between ~18.5 and 16.5 ka with maximum *G. ruber* abundances, which suggests that surface waters were marked by the most subtropical hydrographic conditions (Fig. 8; Moros et al., 2021). As pointed out by Moros et al. (2021), this 2 ka period equivalent to Heinrich Stadial 1 in the Northern Hemisphere is concurrent with widespread Southern Hemisphere and ocean warming (Kaiser et al., 2005; Bereiter et al., 2018), rapid glacier retreat in New Zealand (Putnam et al., 2013), and CO_2 increase (Lourantou et al., 2010). In contrast to the second phase of southward migration of the Subtropical and Subantarctic fronts that took place at the onset of the Holocene (Moros et al., 2021), the first phase of southward displacement between ~18.5 and 16.5 ka is not matched by a change in benthic foraminiferal faunas, suggesting that deep-sea benthic environments were buffered against this event. If shoaling of AABW and greater mixing with overlying waters is indeed responsible for the observed glacial benthic foraminiferal communities, it can be hypothesized that it was not affected by the poleward retreat of Subtropical and Subantarctic fronts during the ~18.5 to 16.5 ka interval.

6. Conclusion

The investigation of benthic foraminiferal assemblages from core MD03-2611 sheds light on the history of deep-sea ecosystems from the Murray Canyons and their response to global climatic patterns during the last 94 ka. Combining our findings to previous knowledge of surface water and terrestrial realms, it is possible to draw the following key conclusions regarding the relationship between deep-sea benthic environments, surface water mass dynamics, and climatic shifts within the terrestrial domain:

- Changes in deep-sea benthic foraminiferal assemblages from the Murray Canyon Group demonstrate a link with global interglacial/glacial cyclicity during the last 94 ka. The dominance of miliolids during glacial periods suggests that conditions at the seafloor were well ventilated and oligotrophic, whereas the abundance of the infaunal *Bolivina variabilis* and *Globocassiculina* spp. points to an overall reduced oxygenation associated with higher food input during the Holocene and MIS 5a-c.
- Benthic foraminiferal assemblages indicate that changes within the deep-sea and continental realms are decoupled during the last 94 ka. During glacial periods, noticeably the Last Glacial Maximum, the outflow of the Murray River transported allochtonous benthic foraminifera from the shelf down to the deep-sea, but did not trigger an increase in organic matter export to deep-sea benthic environments. Likewise, benthic foraminiferal communities do not respond to the glacial increase in aeolian dust input, thus further pointing to a disconnection between continental and deep-sea realms at the core site.
- Foraminiferal communities, noticeably the dominance of the epibenthic *Gavelinopsis praegeri*, evidence a strengthening of bottom-water currents during MIS 1 and MIS 5a-c, possibly triggered by an intensification of the poleward-circulating deep eastern boundary current. Considering planktic and benthic foraminiferal assemblages, the intensification of the deep eastern boundary current appears to follow the arrival of tropical/subtropical surface waters originating from the Indo-Pacific Warm Pool above the core site.
- Bottom-water currents were probably weaker during glacial periods, indicating a dwindling of the deep eastern boundary current. The oxygen-rich and oligotrophic conditions at the seafloor during the last glacial period may reflect a greater shoaling and mixing of oxygen-rich Antarctic Bottom Water with overlying water masses, especially during the Last Glacial Maximum. This change in the bottom-water make up would follow the northward displacement of the Subtropical and Subantarctic fronts and coincide with a withering influence of the Leeuwin Current within surface waters.

Author contributions

RF: Conceptualization, Formal analysis, Writing – original draft, Visualization. PDD: Conceptualization, Writing – review & editing, Supervision, core acquisition and supervision of core processing, Funding acquisition. PD: Investigation (identification and quantification of benthic foraminifera), review and editing. MM: Conceptualization, Investigation (sample preparation and benthic foraminifera picking), review and editing.

Declaration of competing interest

The authors declare that they have no known competing financial interests or personal relationships that could have appeared to influence the work reported in this paper.

Data availability

The benthic foraminiferal data presented in this work together with the clay mineralogy first published by Gingele et al. (2004) are available at the PANGEA online repository following these links: https://doi.org/10.1594/PANGAEA.960585 (benthic foraminiferal census data), https://doi.org/10.1594/PANGAEA.960587 (clay mineralogy). Previously published data used in this study is available following this link: https://doi.org/10.1594/PANGAEA.911846.

10 Acknowledgements

Core MD03-2611 was obtained during the AUSCAN cruise funded by grants from the Australian Research Council (ARC), the ANU Faculty Research Fund and the National Oceans Office, all awarded to PDD. The skills of Yvon Balut in obtaining the core are gratefully acknowledged as well as the French Paul Emile Victor Polar Institute [IPEV] that gave PDD access to the *RV Marion Dufresne II*. We further thank the TANDEM project (Rising star initiative, Pays de la Loire region, France) that provided funding for PD's MSc. Finally, we would like to thank the Editor and the three anonymous reviewers for their constructive feedback and helpful comments.

Appendix A. Supplementary data

Supplementary data to this article can be found online at https://doi.org/10.1016/j.quascirev.2023.108328.

References

Alexander, S.P., DeLaca, T.E., 1987. Feeding adaptations of the foraminiferan *Cibicides refulgens* living epizoically and parasitically on the Antarctic scallop *Adamussium colbecki*. Biol. Bull. 173, 136–159.

Altenbach, A.V., Lutze, G.F., Schiebel, R., Schönfeld, J., 2003. Impact of interrelated and interdependent ecological controls on benthic foraminifera: an example from the Gulf of Guinea. Palaeogeogr. Palaeoclimatol. Palaeoecol. 197, 213–238.

Alve, E., 1991. Foraminifera, climatic change, and pollution: a study of the late Holocene sediments in Drammensfjord, southeast Norway. Holocene 1, 243–261.

Aoki, S., Yamazaki, K., Hirano, D., Katsumata, K., Shimada, K., Kitade, Y., Sasaki, H., Murase, H., 2020. Reversal of freshening trend of antarctic bottom water in the Australian-Antarctic Basin during 2010s. Sci. Rep. 10, 14415.

Arístegui, J., Gasol, J.M., Duarte, C.M., Herndld, G.J., 2009. Microbial oceanography of the dark ocean's pelagic realm. Limnol. Oceanogr. 54 (5), 1501–1529.

Barker, S., Diz, P., Vautravers, M.J., Pike, J., Knorr, G., Hall, I.R., Broecker, W.S., 2009. Interhemispheric Atlantic seesaw response during the last deglaciation. Nature 457, 1097–1102.

Barmawidjaja, D.M., Van der Zwaan, G.J., Jorissen, F.J., Puskaric, S., 1995. 150 years of eutrophication in the northern Adriatic Sea: evidence from a benthic foraminiferal record. Mar. Geol. 122, 367–384.

Basak, C., Rathburn, A.E., Pérez, M.E., Martin, J.B., Kluesner, J.W., Levin, L.A., De Deckker, P., Gieskes, J.M., Abriani, M., 2009. Carbon and oxygen isotope geochemistry of live (stained) benthic foraminifera from the Aleutian Margin and the Southern Australian Margin. Mar. Micropaleontol. 70, 89–101.

Bassinot, F.C., Labeyrie, L.D., Vincent, E., Quidelleur, X., Schackleton, N.J., Lancelot, Y., 1994. The astronomical theory of climate and the age of the Brunhes-Matuyama magnetic reversal. Earth Planet Sci. Lett. 126, 91–108.

Bereiter, B., Shackleton, S., Baggenstos, D., Kawamura, K., Severinghaus, J., 2018. Mean global ocean temperatures during the last glacial transition. Nature 553, 39–44.

Berends, C.J., Köhler, P., Lourens, L.J., Wal, R.S.W., 2021. On the cause of the mid-pleistocene transition. Rev. Geophys. 59, e2020RG000727.

Blaauw, M., Christen, J.A., 2011. Flexible paleoclimate age-depth models using an autoregressive gamma process. Bayesian Analysis 6 (3), 457–474. https://doi.org/10.1214/11-BA618.

Blunier, T., Brook, E.J., 2001. Timing of millenial-scale climate change in Antarctica and Greenland during the last glacial period. Science 291, 109–112.

Bunzel, D., Schmiedl, G., Lindhorst, S., Mackensen, A., Reolid, J., Romahn, S., Betzler, C., 2017. A multi-proxy analysis of Late Quaternary ocean and climate variability for the Maldives, Inner Sea. Clim. Past 13, 1791–1813.

Buzas, M., 1990. Another look at confidence limits for species proportions. J. Paleontol. 64 (5), 842–843.

Cann, J.H., Belperio, A.P., Gostin, V.A., Rice, R.L., 1993. Contemporary benthic foraminifera in gulf st Vincent, South Australia, and a refined late pleistocene sea-level history. Aust. J. Earth Sci. 40, 197–211.

Chapman, F., 1907. Recent Foraminifera off Victoria: some littoral gathering. J. Quekett Microsc. Club 10, 117–146.

Cirano, M., Middleton, J.F., 2004. Aspects of the mean wintertime circulation along Australia's southern shelves: numerical studies. J. Phys. Oceanogr. 34, 668–684.

Clarke, K.R., Gorley, R.N., 2006. PRIMER V6: User Manual/Tutorial (Plymouth Routines in Multivariate Ecological Research). PRIMER-E, Plymouth.

Cohen, T.J., Arnold, L.J., Gázquez, F., May, J.-H., Marx, S.K., Jankowski, N.R., Chivas, A. R., Garćia, A., Cadd, H., Parker, A.G., Jansen, J.D., Fu, X., Waldmann, N., Nanson, G. C., Jones, B.G., Gadd, P., 2022. Late quaternary climate change in Australia's arid interior: evidence from kati Thanda – Lake Eyre. Quat. Sci. Rev. 292, 107635.

Corliss, B.H., 1979. Recent deep-sea benthonic foraminiferal distributions in the southeast Indian Ocean: inferred bottom-water routes and ecological implications. Mar. Geol. 31, 115–138.

Corliss, B.H., Chen, C., 1988. Morphotype patterns of Norwegian Sea deep-sea benthic foraminifera and ecological implications. Geology 16, 716–719.

Corliss, B.H., Martinson, D.G., Keffer, T., 1986. Late Quaternary deep-ocean circulation. GSA Bulletin 97, 1106–1121.

Cresswell, G.R., Domingues, C.M., 2009. The Leeuwin current south of western Australia. J. Roy. Soc. West Aust. 92, 83–100.

Cresswell, G.R., Griffin, D.A., 2004. The Leeuwin Current, eddies and sub-Antarctic waters off south-western Australia. Mar. Freshw. Res. 55, 267–276.

De Deckker, P., Arnold, L.J., van der Kaars, S., Bayon, G., Stuut, J.-B.W., Perner, K., Lopes dos Santos, R., Uemura, R., Demuro, M., 2019. Marine Isotope Stage 4 in Australasia: a full glacial culminating 65,000 years ago – global connections and implications for human dispersal. Quat. Sci. Rev. 204, 187–207.

De Deckker, P., Moros, M., Perner, K., Blanz, T., Wacker, L., Schneider, R., Barrows, T.T., O'Loingsigh, T., Jansen, E., 2020. Climatic evolution in the Australian region over the last 94 ka - spanning human occupancy -, and unveiling the Last Glacial Maximum. Quat. Sci. Rev. 249, 106593.

De Deckker, P., Moros, M., Perner, K., Jansen, E., 2012. Influence of the tropics and southern westerlies on glacial interhemispheric asymmetry. Nat. Geosci. 5, 266–269.

De Deckker, P., van der Kaars, S., Haberle, S., Hua, Q., Stuut, J.B.W., 2021. The pollen record from marine core MD03-2607 from offshore Kangaroo Island spanning the last 125 ka; implications for vegetation changes across the Murray-Darling Basin. Aust. J. Earth Sci. 68, 928–951.

De Rijk, S., Jorissen, F., Rohling, E.J., Troelstra, S.R., 2000. Organic flux control on bathymetric zonation of Mediterranean benthic foraminifera. Mar. Micropaleontol. 40, 151–166.

De Stigter, H.C., Jorissen, F.J., Van der Zwaan, G.J., 1996. Bathymetric distribution and microhabitat partioning of live (Rose Bengal stained) benthic foraminifera along a shelf to deep sea transect in the southern Adriatic Sea. In: De Stigter, H.C. (Ed.), Recent and Fossil Benthic Foraminifera in the Adriatic Sea: Distribution Patterns in Relation to Organic Flux and Oxygen Concentration at the Seabed. Geologica Ultraiectina, pp. 39–69.

Debenay, J.-P., 2012. A Guide to 1,000 Foraminifera from the Southwestern Pacific New Caledonia. IRD Editions, p. 385.

Denton, G.H., 2000. Does an asymmetric thermohaline-ice-sheet oscillator drive 100 000-yr glacial cycles? J. Quat. Sci. 15, 301–318.

Dias, B.B., Barbosa, C.F., Faria, G.R., Seoane, J.C.S., Albuquerque, A.L.S., 2018. The effects of multidecadal-scale phytodetritus disturbances on the benthic foraminiferal community of a Western Boundary Upwelling System, Brazil. Mar. Micropaleontol. 139, 102–112.

Diz, P., Francés, G., Rosón, G., 2006. Effects of contrasting upwelling–downwelling on benthic foraminiferal distribution in the Ría de Vigo (NW Spain). J. Mar. Syst. 60, 1–18.

Duran, E.R., Phillips, H.E., Furue, R., Spence, P., Bindoff, N.L., 2020. Southern Australia Current System based on a gridded hydrography and a high-resolution model. Prog. Oceanogr. 181 (9), 102254.

Durand, M., Mojtahid, M., Maillet, G.M., Proust, J.N., Lehay, D., Ehrhold, A., Barré, A., Howa, H., 2016. Mid- to late-Holocene environmental evolution of the Loire estuary as observed from sedimentary characteristics and benthic foraminiferal assemblages. J. Sea Res. 118, 17–34.

Duros, P., Fontanier, C., de Stigter, H.C., Cesbron, F., Metzger, E., Jorissen, F.J., 2012. Live and dead benthic foraminiferal faunas from Whittard Canyon (NE Atlantic): focus on taphonomic processes and paleo-environmental applications. Mar. Micropaleontol. 94–95, 25–44.

Dutkiewicz, A., Müller, R.D., O'Callaghan, S., Jónasson, H., 2015. Census of seafloor sediments in the world's ocean. Geology 43, 795–798.

Fatela, F., Taborda, R., 2002. Confidence limits of species proportions in microfossil assemblages. Mar. Micropaleontol. 45 (2), 169–174.

Fentimen, R., Feenstra, E., Rüggeberg, A., Vennemann, T., Hajdas, I., Adatte, T., Van Rooij, D., Foubert, A., 2020. Cold-water coral mound archive provides unique insights into intermediate water mass dynamics in the alboran sea during the last deglaciation. Front. Mar. Sci. 7, 354.

Fentimen, R., Schmiedl, G., Rüggeberg, A., Foubert, A., 2021. Benthic foraminiferal faunas associated with cold-water coral environments in the North Atlantic realm. The Depositional Record 7, 223–255.

Fontanier, C., Jorissen, F.J., Chaillou, G., Anschutz, P., Grémare, A., Griveaud, C., 2005. Live foraminiferal faunas from a 2800m deep lower canyon station from the Bay of Biscay: faunal response to focusing of refractory organic matter. Deep Sea Res. Oceanogr. Res. Pap. 52, 1189–1227.

Fontanier, C., Jorissen, F.J., Lansard, B., Mouret, A., Buscail, R., Schmidt, S., Kerhervé, P., Buron, F., Zaragosi, S., Hunault, G., Ernoult, E., Artero, C., Anschutz, P., Rabouille, C., 2008. Live foraminifera from the open slope between grand rhône and petit rhône canyons (gulf of Lions, NW mediterranean). Deep Sea Res. Oceanogr. Res. Pap. 55, 1532–1553.

Garcia, J., Mojtahid, M., Howa, H., Michel, E., Schiebel, R., Charbonnier, C., Anschutz, P., Jorissen, F.J., 2013. Benthic and planktic foraminifera as indicators of late glacial to Holocene paleoclimatic changes in a marginal environment: an example from the southeastern bay of biscay. Acta Protozool. 52, 161–180.

Gingele, F., De Deckker, P., Norman, M., 2007. Late Pleistocene and Holocene climate of SE Australia reconstructed from dust and river loads deposited offshore the River Murray Mouth. Earth Planet Sci. Lett. 255, 257–272.

Gingele, F.X., De Deckker, P., 2005. Late Quaternary fluctuations of palaeoproductivity in the Murray Canyons area, South Australian continental margin. Palaeogeogr. Palaeoclimatol. Palaeoecol. 220, 361–373.

Gingele, F.X., De Deckker, P., Hillenbrand, C.-D., 2004. Late Quaternary terrigenous sediments from the Murray Canyons area, offshore South Australia and their implications for sea level change, palaeoclimate and palaeodrainage of the Murray–Darling Basin. Mar. Geol. 212, 183–197.

Gooday, A.J., 1993. The biology of Deep-Sea foraminifera: a review of some advances and their applications in paleoceanography. Palaios 9, 14–31.

Gooday, A.J., 2019. Deep-Sea benthic foraminifera. In: Cochran, J.K., Bokuniewicz, H.J., Yager, P.L. (Eds.), Encyclopedia of Ocean Sciences, third ed. Academic Press, Oxford, pp. 684–705.

Gooday, A.J., Jorissen, F.J., 2012. Benthic foraminiferal biogeography: controls on global distribution patterns in deep-water settings. Ann. Rev. Mar. Sci 4, 237–262.

Grant, K.M., Rohling, E.J., Bar-Matthews, M., Ayalon, A., Medina-Elizalde, M., Bronk Ramsey, C., Stow, C., Roberts, A.P., 2012. Rapid coupling between ice volume and polar temperature over the past 150,000 years. Nature 491, 744–747.

Grootes, P.M., Stuiver, M., White, J.W.C., Johnsen, S., Jouzel, J., 1993. Comparison of oxygen isotope records from the GISP2 and GRIP Greenland ice cores. Nature 366, 552–554.

Hanson, C.E., Pattiaratchi, C.B., Waite, A.M., 2005. Sporadic upwelling on a downwelling coast: phytoplankton responses to spatially variable nutrient dynamics off the Gascoyne region of Western Australia. Continent. Shelf Res. 25, 1561–1582.

Hays, J.D., Imbrie, J., Shackleton, N.J., 1976. Variations in the Earth's orbit: pacemaker of the ice ages. Science 194, 1121–1132.

Hayward, B., Grenfell, H.R., Reid, C.M., Hayward, K.A., 1999. Recent New Zealand Shallow-Water Benthic Foraminifera: Taxonomy, Ecologic Distribution, Biogeography, and Use in Paleoenvironmental Assessment, vol. 21. GNS Science Monographs, p. 258.
Hayward, B., Grenfell, H.R., Sabaa, A.T., Neil, H.L., Buzas, M.A., 2010. Recent New Zealand deep-water benthic foraminifera: Taxonomy, ecologic distribution, biogeography, and use in paleoenvironmental assessment. GNS Science Monographs 26, 363.
Hayward, B., Hollis, C.J., Grenfell, H.R., 1997. Recent Elphiidiae (Foraminiferida) of the South-West Pacific and Fossil Elphidiidae of New Zealand, vol. 16. GNS Science Monographs, p. 166.
Hayward, B., Sabaa, A.T., Greenfell, H.R., Neil, H., Bostock, H., 2013. Ecological distribution of recent deep-water foraminifera around New Zealand. J. Foraminifer. Res. 43, 415–442.
Hayward, B.W., Grenfell, H.R., Sabaa, A.T., Neil, H.L., 2007. Factors influencing the distribution of Subantarctic deep-sea benthic foraminifera, Campbell and Bounty Plateaux, New Zealand. Mar. Micropaleontol. 62, 141–166.
Hesse, P.P., McTainsh, G.H., 1999. Last glacial maximum to early Holocene wind strength in the mid-latitudes of the southern Hemisphere from aeolian dust in the Tasman sea. Quat. Res. 52, 343–349.
Hill, P.J., De Deckker, P., 2004. AUSCAN seafloor mapping and geological sampling survey on the Australian southern margin. Geoscience Australia Record 2004/04.
Hill, P.J., De Deckker, P., Exon, N.F., 2005. Geomorphology and evolution of the gigantic Murray canyons on the Australian southern margin. Aust. J. Earth Sci. 52, 117–136.
Hill, P.J., De Deckker, P., von der Borch, C., Murray-Wallace, C.V., 2009. Ancestral Murray River on the Lacepede Shelf, southern Australia: late Quaternary migrations of a major river outlet and strandline development. Aust. J. Earth Sci. 56, 135–157.
Imbrie, J., Berger, A., Shackleton, N.J., 1993. Role of orbital forcing: a two-million year perspective. In: Eddy, J.A., Oeschger, H. (Eds.), Global Changes in the Perspective of the Past. John Wiley, Chichester and New York, pp. 263–277.
James, N.P., Bone, Y., 2011. The South Australian sea. In: James, N.P., Bone, Y. (Eds.), Neritic Carbonate Sediments in a Temperate Realm - Southern Australia. Springer Science and Business Media B.V, p. 254.
James, N.P., Bone, Y., Borch, C.C., Gostin, V.A., 1992. Modern carbonate and terrigenous clastic sediments on a cool water, high energy, mid-latitude shelf: Lacepede, southern Australia. Sedimentology 39, 877–903.
Jorissen, F.J., de Stigter, H.C., Widmark, J.G., 1995. A conceptual model explaining benthic foraminiferal microhabitats. Mar. Micropaleontol. 26, 3–15.
Jorissen, F.J., Fontanier, C., Thomas, E., 2007. Chapter Seven Paleoceanographical Proxies Based on Deep-Sea Benthic Foraminiferal Assemblage Characteristics, Proxies in Late Cenozoic Paleoceanography, pp. 263–325.
Jouzel, J., Masson-Delmotte, V., Cattani, O., Dreyfus, G., Falourd, S., Hoffmann, G., Minster, B., Nouet, J., Barnola, J.M., Chappellaz, J., Fischer, H., Gallet, J.C., Johnsen, S., Leuenberger, M., Loulergue, L., Luethi, D., Oerter, H., Parrenin, F., Raisbeck, G., Raynaud, D., Schilt, A., Schwander, J., Selmo, E., Souchez, R., Spahni, R., Stauffer, B., Steffensen, J.P., Stenni, B., Stocker, T.F., Tison, J.L., Werner, M., Wolff, E.W., 2007. Orbital and millennial antarctic climate variability over the past 800,000 years. Science 317, 793–796.
Kaiser, J., Lamy, F., Hebbeln, D., 2005. A 70-kyr sea surface temperature record off southern Chile (Ocean Drilling Program Site 1233). Paleoceanography 20, PA4009.
Koho, K.A., García, R., de Stigter, H.C., Epping, E., Koning, E., Kouwenhoven, T.J., van der Zwaan, G.J., 2008. Sedimentary labile organic carbon and pore water redox control on species distribution of benthic foraminifera: a case study from Lisbon–Setúbal Canyon (southern Portugal). Prog. Oceanogr. 79, 55–82.
Kuijpers, A., Troelstra, S.R., Prins, M.A., Linthout, K., Akhmetzhanov, A., Bouryak, S., Bachmann, M.F., Lassen, S., Rasmussen, S., Jensen, J.B., 2003. Late Quaternary sedimentary processes and ocean circulation changes at the Southeast Greenland margin. Mar. Geol. 195, 109–129.
Lambeck, K., Rouby, H., Purcell, A., Sun, Y., Sambridge, M., 2014. Sea level and global ice volumes from the last glacial maximum to the Holocene. Proceed. Nat. Acad. Sci. USA 111, 15296–15303.
Langer, M.R., 2008. Assessing the contribution of foraminiferan protists to global ocean carbonate production. J. Eukaryot. Microbiol. 55, 163–169.
Lewis, R., 1981. Seasonal upwelling along the south-eastern coastline of South Australia. Mar. Freshw. Res. 32, 843–854.
Li, Q., McGowran, B., James, N.P., Bone, Y., 1996. Foraminiferal biofacies on the mid-latitude Lincoln Shelf, South Australia: oceanographic and sedimentological implications. Mar. Geol. 129, 285–312.
Lisiecki, L.E., Raymo, M.E., 2005. A Pliocene-Pleistocene stack of 57 globally distributed benthic δ18O records. Paleoceanography 20, PA1003.
Liesicki, L.E., Stern, J.V., 2016. Regional and global benthic δ18O stacks for the last glacial cycle. Paleoceanogr. Paleoclimatol. 31 (10).
Lourantou, A., Lavrič, J.V., Köhler, P., Barnola, J.-M., Paillard, D., Michel, E., Raynaud, D., Chappellaz, J., 2010. Constraint of the CO2 rise by new atmospheric carbon isotopic measurements during the last deglaciation. Global Biogeochem. Cycles 24, GB2015.
Lowe, J., Walker, M., 2014. Reconstructing Quaternary Environments, 3 ed. Routledge, London and New York, p. 568.
Magee, J.W., Miller, G.H., Spooner, N.A., Questiaux, D., 2004. Continuous 150 k.y. monsoon record from Lake Eyre, Australia: insolation-forcing implications and unexpected Holocene failure. Geology 32 (10), 885–888.
Martins, M.V., Quintino, V., Tentugal, R.M., Frontalini, F., Miranda, P., Mattos Laut, L.L., Martins, R., Rodrigues, A.M., 2015. Characterization of bottom hydrodynamic conditions on the central western Portuguese continental shelf based on benthic foraminifera and sedimentary parameters. Mar. Environ. Res. 109, 52–68.
McCave, I.N., 2008. Size sorting during transport and deposition of fine sediments: sortable silt and flow speed. In: Rebesco, M., Camerlenghi, A. (Eds.), Contourites. Elsevier, Amsterdam, pp. 379–407.
McCartney, M.S., 1977. Subantarctic Mode water. In: Angel, M.V. (Ed.), A Voyage of Discovery, vol. 24, pp. 103–119.
McCartney, M.S., 1982. The subtropical recirculation of Mode Waters. J. Mar. Res. 40, 427–464.
McDonagh, E.L., Bryden, H.L., King, B.A., Sanders, R.J., 2008. The circulation of the Indian Ocean at 32°S. Prog. Oceanogr. 79, 20–36.
Messié, M., Ledesma, J., Kolber, D.D., Michisaki, R.P., Foley, D.G., Chavez, F.P., 2009. Potential new production estimates in four eastern boundary upwelling ecosystems. Prog. Oceanogr. 83, 151–158.
Middleton, J.F., Cirano, C., 2002. A northern boundary current along Australia's southern shelves: the Flinders Current. J. Geophys. Res. 107 (C9), 3129.
Middleton, J.F., Bye, J.A.T., 2007. A review of the shelf-slope circulation along Australia's southern shelves: Cape Leeuwin to Portland. Prog. Oceanogr. 75, 1–41.
Miguez-Salas, O., Rodríguez-Tovar, F.J., De Weger, W., 2020. *Macaronichnus* and contourite depositional settings: bottom currents and nutrients as coupling factors. Palaeogeogr. Palaeoclimatol. Palaeoecol. 545, 109639.
Miller, G.H., Brigham-Grette, J., Alley, R.B., Anderson, L., Bauch, H.A., Douglas, M.S.V., Edwards, M.E., Elias, S.A., Finney, B.P., Fitzpatrick, J.J., Funder, S.V., Herbert, T.D., Hinzman, L.D., Kaufman, D.S., MacDonald, G.M., Polyak, L., Robock, A., Serreze, M. C., Smol, J.P., Spielhagen, R., White, J.W.C., Wolfe, A.P., Wolff, E.W., 2010. Temperature and precipitation history of the Arctic. Quat. Sci. Rev. 29 (15–16), 1679–1715.
Moine, O., Rousseau, D.-D., Antoine, P., 2008. The impact of Dansgaard–Oeschger cycles on the loessic environment and malacofauna of Nussloch (Germany) during the Upper Weichselian. Quat. Res. 70, 91–104.
Mojtahid, M., Jorissen, F.J., Garcia, J., Schiebel, R., Michel, E., Eynaud, F., Gillet, H., Cremer, M., Diz Ferreiro, P., Siccha, M., Howa, H., 2013. High resolution Holocene record in the southeastern Bay of Biscay: global versus regional climate signals. Palaeogeogr. Palaeoclimatol. Palaeoecol. 377, 28–44.
Mojtahid, M., Michel, E., De Deckker, P., 2020. From "source to sink" – a new perspective on the past dynamics of the Murray Canyon Group from benthic foraminiferal communities. Mar. Micropaleontol. 160, 101877.
Moros, M., De Deckker, P., Jansen, E., Perner, K., Telford, R.J., 2009. Holocene climate variability in the Southern Ocean recorded in a deep-sea sediment core off South Australia. Quat. Sci. Rev. 28, 1932–1940.
Moros, M., De Deckker, P., Perner, K., Ninnemann, U.S., Wacker, L., Telford, R., Jansen, E., Blanz, T., Schneider, R., 2021. Hydrographic shifts south of Australia over the last deglaciation and possible interhemispheric linkages. Quat. Res. 102, 130–141.
Mullineaux, L.S., Lohmann, G.P., 1981. Late Quaternary stagnations and recirculation of the eastern Mediterranean: changes in the deep water recorded by fossil benthic foraminifera. J. Foraminifer. Res. 11 (1), 20–39.
Murgese, D.S., De Deckker, P., 2005. The distribution of deep-sea benthic foraminifera in core tops from the eastern Indian Ocean. Mar. Micropaleontol. 56, 25–49.
Murray, J.W., 1970. Foraminifers of the western approaches to the English channel. Micropaleontology 16, 471–485.
Murray, J.W., 2006. Ecology and Applications of Benthic Foraminifera. Cambridge University Press, Cambridge, p. 440.
Nash, G.J., Binnie, M.N., Cann, J.H., 2010. Distribution of foraminifera and ostracods in the onkaparinga estuary, South Australia. Aust. J. Earth Sci. 57, 901–910.
Nash, G.J., De Deckker, P., Mitchell, C., Murray-Wallace, C.V., Hua, Q., 2018. Micropalaeontological evidence for deglacial marine flooding of the ancient courses of the River Murray across the Lacepede Shelf, southern Australia. Mar. Micropaleontol. 141, 55–72.
Nees, S., Armand, L., De Deckker, P., Labracherie, M., Passlow, V., 1999. A diatom and benthic foraminiferal record from the South Tasman Rise (southeastern Indian Ocean): implications for palaeoceanographic changes for the last 200,000 years. Mar. Micropaleontol. 38, 69–89.
Orsi, A.H., Smethie, W.M., Bullister, J.L., 2002. On the total input of Antarctic waters to the deep ocean: a preliminary estimate from chlorofluorocarbon measurements. J. Geophys. Res. 107 (C8).
Osborn, N.L., CiesielskiI, P.F., Ledbetter, M.T., 1983. Disconformities and paleoceanography in the southeast Indian Ocean during the past 5.4 million years. GSA Bulletin 94, 1345–1358.
Parr, W.J., 1932. Victorian and South Australian shallow-water foraminifera. Proc. Roy. Soc. Vic. 44, 1–14.
Passlow, V., Pinxian, W., Chivas, A.R., 1997. Late Quaternary palaeoceanography near Tasmania, southern Australia. Palaeogeogr. Palaeoclimatol. Palaeoecol. 131, 433–463.
Past Interglacials Working Group of PAGES, 2016. Interglacials of the last 800,000 years. Rev. Geophys. 54, 162–219. https://doi.org/10.1002/2015RG000482.
Perner, K., Moros, M., De Deckker, P., Blanz, T., Wacker, L., Telford, R., Siegel, H., Schneider, R., Jansen, E., 2018. Heat export from the tropics drives mid to late Holocene palaeoceanographic changes offshore southern Australia. Quat. Sci. Rev. 180, 96–110.
Peterson, L.C., 1984. Recent abyssal benthic foraminiferal biofacies of the eastern equatorial Indian Ocean. Mar. Micropaleontol. 8, 479–519.
Piola, A.R., Georgi, D.T., 1982. Circumpolar properties of antarctic intermediate water and subantarctic Mode water. Deep-Sea Res. 29, 687–711.
Putnam, A.E., Schaefer, J.M., Denton, G.H., Barrell, D.J.A., Andersen, B.G., Koffman, T. N.B., Rowan, A.V., Finkel, R.C., Rood, D.H., Schwartz, R., Vandergoes, M.J., Plummer, M.A., Brocklehurst, S.H., Kelley, S.E., Ladig, K.L., 2013. Warming and

glacier recession in the rakaia valley, southern alps of New Zealand, during Heinrich stadial 1. Earth Planet Sci. Lett. 382, 98–110.
Pye, K., 1995. The nature, origin and accumulation of loess. Quat. Sci. Rev. 14, 653–667.
Quilty, P.G., Hosie, G., 2006. Modern foraminifera, Swan River estuary, western Australia: distribution and controlling factors. J. Foraminifer. Res. 36, 291–314.
R Team, 2022. R: A Language and Environment for Statistical Computing. Vienna, Austria.
Rathburn, A.E., Corliss, B.H., 1994. The ecology of living (stained) deep-sea from the Sulu Sea. Paleoceanography 9, 87–150.
Rebesco, M., Hernández-Molina, F.J., Van Rooij, D., Wåhlin, A., 2014. Contourites and associated sediments controlled by deep-water circulation processes: state-of-the-art and future considerations. Mar. Geol. 352, 111–154.
Reeves, J.M., Barrows, T.T., Cohen, T.J., Kiem, A.S., Bostock, H.C., Fitzsimmons, K.E., Jansen, J.D., Kemp, J., Krause, C., Petherick, L., Phipps, S.J., 2013. Climate variability over the last 35,000 years recorded in marine and terrestrial archives in the Australian region: an OZ-INTIMATE compilation. Quat. Sci. Rev. 74, 21–34.
Reimer, P.J., Austin, W.E.N., Bard, E., Bayliss, A., Blackwell, P.G., Bronk Ramsey, C., Butzin, M., Cheng, H., Lawrence Edwards, R., Friedrich, M., Grootes, P.M., Guilderson, T.P., Hajdas, I., Heaton, T., Hogg, A.G., Hughen, K.A., Kromer, B., Manning, S.W., Muscheler, R., Palmer, J.G., Pearson, C., Van der Plicht, J., Reimer, R.W., Richards, D.A., Marian Scott, E., Southon, J.R., Turner, C.S.M., Wacker, L., Adolphi, F., Büntgen, U., Capano, M., Fahrni, S.M., Fogtmann-Schulz, A., Friedrich, R., Köhler, P., Kudsk, S., Miyake, F., Olsen, J., Reinig, F., Sakamoto, M., Sookdeo, A., Talamo, S., 2020. The IntCal20 northern Hemisphere radiocarbon age calibration curve (0–55 cal kBP). Radiocarbon 62 (4), 725–757. https://doi.org/10.1017/RDC.2020.4.
Reimer, P.J., Bard, E., Bayliss, A., Beck, J.W., Blackwell, P.G., Bronk Ramsey, C., et al., 2013. IntCal13 and MARINE013 radiocarbon age calibration curves 0-50000 year. Radiocarbon 55, 1869e1887.
Richardson, L.E., Middleton, J.F., James, N.P., Kyser, T.K., Opdyke, B.N., 2020. Upwelling characteristics and nutrient enrichment of the Kangaroo Island upwelling region, South Australia. Continent. Shelf Res. 200, 104111.
Richardson, L.E., Middleton, J.F., Kyser, T.K., James, N.P., Opdyke, B.N., 2019. Shallow water masses and their connectivity along the southern Australian continental margin. Deep Sea Res. Oceanogr. Res. Pap. 152, 103083.
Ridgway, K.R., Condie, S.A., 2004. The 5500-km-long boundary flow off western and southern Australia. J. Geophys. Res. 109, C04017.
Rintoul, S.R., 1998. On the origin and influence of Adelie land bottom water. In: Jacobs, S.S., Weiss, R.F. (Eds.), Ocean, Ice, and Atmosphere: Interactions at the Antarctic Continental Margin. AGU, Washington DC, pp. 151–171.
Rochford, D., 1986. Seasonal changes in the distribution of Leeuwin current waters of southern Australia. Aust. J. Mar. Freshw. Res. 37, 1–10.
Saidova, K.M., 2008. Benthic foraminifera communities of the andaman sea (Indian ocean). Oceanology 48, 517–523.
Saupe, A., Schmidt, J., Petersen, J., Bahr, A., Dias, B.B., Albuquerque, A.L.S., Díaz Ramos, R.A., Grunert, P., 2022. Controlling parameters of benthic Deep-Sea foraminiferal biogeography at the Brazilian continental margin (11-22°S). Front. Mar. Sci. 9, 901224.
Schmiedl, G., Mitschele, A., Beck, S., Emeis, K.-C., Hemleben, C., Schulz, H., Sperling, M., Weldeab, S., 2003. Benthic foraminiferal record of ecosystem variability in the eastern Mediterranean Sea during times of sapropel S5 and S6 deposition. Palaeogeogr. Palaeoclimatol. Palaeoecol. 190, 139–164.
Schönfeld, J., 1997. The impact of the Mediterranean Outflow Water (MOW) on benthic foraminiferal assemblages and surface sediments at the southern Portuguese continental margin. Mar. Micropaleontol. 29, 211–236.
Schönfeld, J., Dullo, W.-C., Pfannkuche, O., Freiwald, A., Rüggeberg, A., Schmidt, S., Weston, J., 2011. Recent benthic foraminiferal assemblages from cold-water coral mounds in the Porcupine Seabight. Facies 57, 187–2013.
Schönfeld, J., Zahn, R., 2000. Late Glacial to Holocene history of the Mediterranean Outflow. Evidence from benthic foraminiferal assemblages and stable isotopes at the Portuguese margin. Palaeogeogr. Palaeoclimatol. Palaeoecol. 159, 85–111.
Schröder-Adams, C.J., Boyd, R., Ruming, K., Sandstrom, M., 2008. Influence of sediment transport dynamics and ocean floor morphology on benthic foraminifera, offshore Fraser Island, Australia. Mar. Geol. 254, 47–61.
Seidov, D., Haupt, B.J., 1997. Global ocean thermohaline conveyor at present and in the Late Quaternary. Geophys. Res. Lett. 24 (22), 2817–2820.
Seiler, W.C., 1975. Tiefenverteilung benthischer Foraminiferen am portugiesischen Kontinentalhang, Meteor Forschungsergebnisse, Deutsche Forschungsgemeinschaft, Reihe C Geologie und Geophysik. Gebrüder Bornträger, Berlin, Stuttgart, pp. 47–94.
Sen Gupta, B.K., Lee, R.F., May, M.S., 1981. Upwelling and an unusual assemblage of benthic foraminifera on the northern Florida continental slope. J. Paleontol. 55, 853–857.
Singh, A.D., Holbourn, A., Kuhnt, W., 2023. Editorial preface to special issue: recent advances in Indian Ocean paleoceanography and paleoclimate. Palaeogeogr. Palaeoclimatol. Palaeoecol. 615, 111443.
Skinner, L.C., Fallon, S., Waelbroeck, C., Michel, E., Barker, S., 2010. Ventilation of the deep southern Ocean and deglacial CO2 rise. Science 328, 1147–1151.
Smart, C.W., Waelbroeck, C., Michel, E., Mazaud, A., 2010. Benthic foraminiferal abundance and stable isotope changes in the Indian Ocean sector of the Southern Ocean during the last 20 kyr: paleoceanographic implications. Palaeogeogr. Palaeoclimatol. Palaeoecol. 297, 537–548.
Smith, A.J., Gallagher, S.J., 2003. The Recent foraminifera and facies of the Bass Canyon: a temperate submarine canyon in Gippsland, Australia. J. Micropaleontol. 22, 63–83.
Smith, D.E., Harrison, S., Firth, C.R., Jordan, J.T., 2011. The early Holocene sea level rise. Quat. Sci. Rev. 30, 1846–1860.
Spindler, M., 1980. The pelagic gulfweed *Sargassum natans* as a habitat for the benthic Foraminifera *Planorbulina acervalis* and *Rosalina globularis*. Neues Jahrbuch für Geologie und Paläontologie 9, 569–580.
Sprigg, R.C., 1948. Newly discovered submarine canyons of new Guinea and southSouth Australia. Nature 161, 246–247.
Stott, L., Timmermann, A., Thunell, R., 2007. Southern Hemisphere and deep-sea warming led deglacial atmospheric CO2 rise and tropical warming. Science 318, 435–438.
Stow, D., 1982. Bottom currents and contourites in the north Atlantic. (I.G.B.A.). Bull. Inst. Geol. Bassin Aquitaine 31, 151–166.
Stow, D., Smillie, Z., Esentia, I., 2019. In: Kirk Cochran, J., Bokuniewicz, H.J., Yager, P.L. (Eds.), Deep-sea Bottom Currents: Their Nature and Distribution. Encyclopedia of Ocean Sciences, third ed., pp. 90–96.
Stow, D., Smillie, Z., 2020. Distinguishing between deep-water sediment facies: turbidites, contourites and hemipelagites. Geosciences 10, 68.
Stuiver, M., Reimer, P.J., 1993. Extended 14C data base and revised CALIB 3.0 14C age calibration program. Radiocarbon 35, 215–230.
Suhr, S.B., Pond, D.W., Gooday, A.J., Smith, C.R., 2003. Selective feeding by benthic foraminifera on phytodetritus on the western Antarctic Peninsula shelf: evidence from fatty acid biomarker analysis. Mar. Ecol. Prog. Ser. 262, 153–162.
Tamsitt, V., Talley, L.D., Mazloff, M.R., 2019. A deep eastern boundary current carrying Indian deep water south of Australia. J. Geophys. Res.: Oceans 124, 2218–2238.
Thomsen, L., Van Weering, T., Gust, G., 2002. Processes in the benthic boundary layer at the Iberian continental margin and their implication for carbon mineralization. Prog. Oceanogr. 52, 315–329.
Van Marle, L.J., 1988. Bathymetric distribution of benthic foraminifera on the Australian-Irian Jaya continental margin, eastern Indonesia. Mar. Micropaleontol. 13, 97–152.
Van Ruth, P.D., Patten, N.L., Doubell, M.J., Chapman, P., Redondo Rodriguez, A., Middleton, J.F., 2018. Seasonal- and event-scale variations in upwelling, enrichment and primary productivity in the eastern Great Australian Bight. Deep Sea Res. Part II Top. Stud. Oceanogr. 157–158, 36–45.
Ward, T.M., McLeay, L.J., Dimmlich, W.F., Rogers, P.J., McClatchie, S.A.M., Matthews, R., Kampf, J., Van Ruth, P.D., 2006. Pelagic ecology of a northern boundary current system: effects of upwelling on the production and distribution of sardine (Sardinops sagax), anchovy (Engraulis australis) and southern bluefin tuna (Thunnus maccoyii) in the Great Australian Bight. Fish. Oceanogr. 15, 191–207.
Weston, J.F., 1982. Distribution and Ecology of Recent Deep Sea Benthic Foraminifera in the Northeast Atlantic Ocean. University of Exeter, p. 442.
Weston, J.F., 1985. Comparison between recent benthic foraminiferal faunas of the porcupine Seabight and western approaches continental slope. J. Micropaleontol. 4, 165–183.
Wickham, H., 2016. ggplot2: Elegant Graphics for Data Analysis. Springer-Verlag, New York.
Wijffels, S.E., Beggs, H., Griffin, C., Middleton, J.F., Cahill, M., King, E., Jones, E., Feng, M., Benthuysen, J.A., Steinberg, C.R., Sutton, P., 2018. A fine spatial-scale sea surface temperature atlas of the Australian regional seas (SSTAARS): seasonal variability and trends around Australasia and New Zealand revisited. J. Mar. Syst. 187, 156–196.
Willingham, J., 2014. The Ecology and Morphology of Deep-Sea Benthic Foraminifera: the Australian Margin and Epifaunal Pore Characteristics. Department of Earth and Environmental Systems. Indiana State University, p. 24.
Woodyer, K.D., 1978. Eolian contributions to marine sediments. J. Sediment. Petrol. 45, 520–529.
Yao, W., Shi, J., 2017. Pacific-Indian interocean circulation of the antarctic intermediate water around South Australia. Acta Oceanol. Sin. 36, 4–14.